

## Biochemical characterization and essentiality of *Plasmodium* fumarate hydratase

Vijay Jayaraman<sup>1</sup>, Arpitha Suryavanshi<sup>1</sup>, Pavithra Kalale<sup>1</sup>, Jyothirmayi Kunala<sup>1,2</sup>, Hemalatha Balaram<sup>1#</sup>

<sup>1</sup> Molecular Biology and Genetics Unit, Jawaharlal Nehru Centre for Advanced Scientific Research (JNCASR), Jakkur P.O., Bengaluru, Karnataka, 560064, INDIA.

Tel: 91-80-22082812 Fax:91-80-22082766

<sup>2</sup> Current affiliation: Molecular characterization/Analytical group, Biocon Research Ltd.-SEZ unit, Biocon Park, Bommasandra-Jigani link road, Bangalore, 560099, INDIA.

#E-mail: [hb@jncasr.ac.in](mailto:hb@jncasr.ac.in)

### SUMMARY

*Plasmodium falciparum* (Pf), the causative agent of malaria has an iron-sulfur cluster-containing class I fumarate hydratase (FH) that catalyzes the interconversion of fumarate to malate, a well-known reaction in the tricarboxylic acid cycle. In humans, the same reaction is catalyzed by class II FH that has no sequence or structural homology with the class I enzyme. Fumarate, generated in large quantities in the parasite as a byproduct of AMP synthesis is converted to malate by the action of FH, and subsequently used in the generation of the key metabolites oxaloacetate, aspartate and pyruvate. Here we report on the kinetic characterization of purified recombinant PfFH, functional complementation of *fh* deficiency in *Escherichia coli* and mitochondrial localization in the parasite. The substrate analog, mercaptosuccinic acid was found to be a potent inhibitor of PfFH with a  $K_i$  value in the nanomolar range. Attempts at knockout of the *fh* gene in *P. berghei* yielded parasite with either wrong integration of the selectable marker cassette or right integration in the background of *fh* gene duplication highlighting the essentiality of FH for the parasite.

### KEY WORDS

*Plasmodium falciparum*, Class I fumarate hydratase, substrate promiscuity, mitochondrial localization, functional complementation, inhibition by mercaptosuccinic acid, fumarase knockout in *P. berghei*

## INTRODUCTION

*Plasmodium falciparum* (Pf), the causative agent of the most lethal form of malaria, during its intraerythrocytic asexual stages derives ATP primarily from glycolysis with low contribution from mitochondrial pathways (1, 2). Bulk of the pyruvate formed is converted to lactic acid with a minor amount entering the tricarboxylic acid (TCA) cycle, the flux through which is upregulated in sexual stages (2). Key intermediates that anaplerotically feed into the TCA cycle are  $\alpha$ -ketoglutarate derived from glutamate, oxaloacetate (OAA) from phosphoenolpyruvate, and fumarate from adenosine 5'-monophosphate (AMP) synthesis. Synthesis of AMP in the parasite is solely from inosine-5'-monophosphate (IMP) through a pathway involving the enzymes adenylosuccinate synthetase (ADSS) and adenylosuccinate lyase (ASL). The net reaction of ADSS and ASL involves consumption of GTP and aspartate and, generation of GDP,  $P_i$  and fumarate. In the rapidly dividing parasite with an AT-rich genome and high energy requirements, leading to a high demand for adenine pools, one would expect a high flux of fumarate generation. The parasite does not secrete fumarate but instead the carbon derived from this metabolite can be traced in malate, OAA, aspartate, pyruvate (through PEP) and lactate (3). The metabolic significance of this fumarate anaplerosis is still obscure. In this context, fumarate hydratase (FH, fumarase) the key enzyme to metabolize fumarate becomes an important candidate for further investigation.

Fumarate hydratase (fumarase, E.C. 4.2.1.2) catalyzes the reversible conversion of fumarate to malate. The stereospecific reaction involves the *anti*-addition of a water molecule across the carbon-carbon double bond of fumarate resulting in the formation of S-malate (L-malate). The reverse reaction proceeds with the elimination of a molecule of water from malate in an *anti*-fashion (4–6). FH comes in two biochemically distinct forms; class I FH a thermolabile, oxygen sensitive, 4Fe-4S cluster containing enzyme and, class II FH, a stable, oxygen insensitive and iron-independent enzyme (7). Class I FH is further divided into two types, two-subunit and single-subunit, depending on the number of genes that encode the functional enzyme (8). There is no sequence homology between these two classes of enzymes. Class I fumarases display substrate promiscuity; apart from catalyzing the interconversion of fumarate and malate, these enzymes also interconvert S,S-tartrate and oxaloacetate and, mesaconate and S-citramalate with varying catalytic efficiencies (9, 10). The 4Fe-4S cluster is bound to the enzyme by 3

metal-thiolate bonds formed between 3 conserved cysteine residues in the protein and 3 ferrous ions (11). The fourth iron in the cluster proposed to be held loosely by a hydroxyl ion, is thought to be directly involved in substrate binding and catalysis as seen in the enzyme aconitase(12, 13).

Both classes of FHs are distributed in all three domains of life with class I FH being more prevalent in archaea, prokaryotes and lower eukaryotes. Many organisms have genes corresponding to both the classes, as in *Escherichia coli* (Ec), which has three FH encoding genes viz., *fum A*, *B* and *C*. Fum A and fum B are 4Fe-4S cluster containing class I enzymes, while Fum C belongs to class II type FH. Recently, another gene *fum D* has been identified in the *E. coli* genome to code for a class I fumarase with altered substrate preferences (14).

The structural and biochemical characteristics of class II FH are thoroughly studied from different organisms viz., human, porcine, yeast, *E. coli* and other sources (15–19). Class I FH, on the other hand, is not as well studied, primarily because of its thermolabile and oxygen sensitive nature. All Apicomplexans and Kinetoplastids possess only class I FH, whereas Dinoflagellates have both classes (20). Biochemical characterization of class I FH from *Leishmania major* (Lm) and *Trypanosoma cruzi*, both Kinetoplastids (18f, 19), and the 3-dimensional structure of LmFH II (11) are the only reports of class I FH from eukaryotes. All *Plasmodium* species have one gene annotated putatively as fumarate hydratase that remains to be characterized. Genetic investigations on the role of TCA cycle enzymes in *P. falciparum* have revealed non-essentiality of all genes of TCA cycle except FH and malate-quinone oxidoreductase (23). Recently, a metabolic network reconstruction of pathways in artemesinin resistant *P. falciparum* strains have identified FH reaction as uniquely essential to these parasites (24). Biochemical characterization of PfFH could throw light on unique features of the enzyme and also provide leads for development of inhibitors.

We report here the kinetic characterization and substrate promiscuity of PfFH, studied using *in vitro* assays on the recombinant enzyme and *E. coli* based functional complementation. DL-mercaptosuccinic acid (DL-MSA), a malate analog was found to be a competitive inhibitor of the *P. falciparum* enzyme. DL-MSA inhibited the growth of  $\Delta$ *fumACB* strain of *E. coli* expressing PfFH as well as the asexual intra-erythrocytic stages of *P. falciparum* in *in vitro* cultures. Attempts at generating *fh* null *P. berghei* yielded drug resistant clonal populations that had

retained the *fh* gene, implying its essentiality.

## EXPERIMENTAL PROCEDURES

### Reagents

RPMLI-1640, components of cytomix and all chemical reagents used were obtained from Sigma Aldrich., USA. MitoTracker CM-H<sub>2</sub>XRos, Hoechst 33342, AlbuMAX I, Ni-NTA conjugated agarose and Phusion high-fidelity DNA polymerase were procured from Thermo Fisher Scientific Inc., USA. Restriction enzymes and T4 DNA ligase were from New England Biolabs, USA. Primers were custom synthesized from Sigma-Aldrich, Bangalore. Media components were from Himedia Laboratories, Mumbai, India. 2, 3-[<sup>13</sup>C]-fumarate was procured from Isotec, Sigma Aldrich, USA and DL-mercaptosuccinic acid (DL-MSA) was obtained from Sigma Aldrich, USA.

### Sequence analysis

*E. coli* FumA (EcFumA) protein sequence (Uniprot ID: P0AC33) was used as query in BLASTP (25) to retrieve all eukaryotic class I FH sequences by restricting the search to eukaryotes. Each of these eukaryotic organisms with class I FH was individually searched for the presence of class II FH using BLASTP and *E. coli* FumC (EcFumC) (Uniprot ID:P05042) as the query sequence. Hits with an e-value lower than  $10^{-10}$  were considered significant.

### Generation of plasmid constructs

Sequences of all oligonucleotide primers used for cloning and for genotyping of *E. coli* and *Plasmodium* mutants are given in **Supplementary Table T1**. For recombinant-expression of PfFH, the DNA fragment corresponding to a protein segment lacking the N-terminal 40 amino acids ( $\Delta 40$ ) was amplified by PCR using parasite genomic DNA as template, appropriate oligonucleotides and Phusion DNA polymerase. The fragment was cloned into modified pET21b (Novagen, Merck, USA) using restriction enzyme sites BamHI and Sall, to obtain the construct pET-PfFH $\Delta 40$  that encodes the protein with an N-terminal (His)<sub>6</sub>-tag. For functional complementation in the *fh* null strain of *E. coli*, pQE30 plasmid (Qiagen, Germany) containing full length (PfFHFL) and two different N-terminus deleted constructs (PfFH $\Delta 40$ , PfFH $\Delta 120$ ) of the *P. falciparum fh* gene were used. The generation of different expression constructs involved amplification by PCR of appropriate

fragments followed by cloning into pQE30 plasmid using restriction sites BamHI and Sall. The plasmids thus obtained are pQE-PfFHFL, pQE-PfFH $\Delta$ 40 and pQE-PfFH $\Delta$ 120. For 3'-tagging of the endogenous *fh* gene with GFP in the *P. falciparum* strain PM1KO (26), the nucleotide fragment corresponding to the full length *fh* gene without the terminator codon was amplified from *P. falciparum* 3D7 genomic DNA using appropriate oligonucleotides (PfFHpGDB-Xho1-FP and PfFHpGDB-AvrII-RP; **Supplementary Table 1**) and cloned into the plasmid, pGDB (26) using the restriction sites XhoI and AvrII. This plasmid construct is referred to as pGDB-PfFH. For recombinant expression of *E. coli* FumC and FumA enzymes, the nucleotide sequence corresponding to the full length genes were PCR amplified using *E. coli* genomic DNA as template and cloned in pQE30 and pET-DUET (Novagen, Merck), respectively using the restriction sites BamHI and Sall. The resulting plasmids are pQE-EcFumC and pET-EcFumA. All the clones were confirmed by DNA sequencing.

### **Protein expression, purification and reconstitution of iron-sulfur cluster**

For recombinant expression of PfFH $\Delta$ 40 and EcFumA, the *E. coli* strain BL21(DE3)-RIL was transformed with pET-PfFH $\Delta$ 40/ pET-EcFumA and selected on Luria-Bertani agar (LB agar) plate containing ampicillin (100  $\mu$ g ml<sup>-1</sup>) and chloramphenicol (34  $\mu$ g ml<sup>-1</sup>). Multiple colonies were picked and inoculated into 10 ml of LB broth. The culture was grown for 6 h at 37 °C, the cells were pelleted, washed with antibiotic free LB broth and then used for inoculating 800 ml of Terrific broth (TB). The cells were grown at 30 °C until OD<sub>600</sub> reached 0.5, thereafter induced with IPTG (0.05 mM for PfFH $\Delta$ 40 and 0.3 mM for EcFumA) and grown for further 16 h at 16 °C for PfFH $\Delta$ 40 and 4 h at 30 °C for EcFumA. Cells were harvested by centrifugation and resuspended in lysis buffer containing 50 mM Tris HCl, pH 7.4, 150 mM NaCl, 1 mM PMSF, 5 mM  $\beta$ -mercaptoethanol and 10 % glycerol. Cell lysis was achieved by 4 cycles of French press at 1000 psi and the lysate cleared by centrifugation at 30,000 x g for 30 minutes. The supernatant was mixed with 1 ml of Ni-NTA agarose slurry pre-equilibrated with lysis buffer and incubated in an anaerobic chamber for 30 minutes at room temperature. The tube was sealed air-tight within the chamber and transferred to 4 °C. Binding of the (His)<sub>6</sub>-tagged PfFH $\Delta$ 40/EcFumA to Ni-NTA agarose was continued with gentle shaking for 3 h. The tube was transferred back to the chamber and the beads were washed with 50 ml of lysis buffer followed by washes with 10 mM and 20 mM imidazole containing lysis buffer (10 ml each) and

the protein eluted directly with 500 mM imidazole in lysis buffer. Equal volume of 100 % glycerol was added to the eluate such that the final concentration of glycerol is 50 %. EcFumC was purified in aerobic conditions using Ni-NTA affinity chromatography.

Reconstitution of the cluster in PffH $\Delta$ 40 and EcFumA was performed under anaerobic conditions. For PffH $\Delta$ 40, the procedure was initiated by incubation of the protein solution with 5 mM DTT for 30 min. Following this, 0.5 mM each of sodium sulfide and ferrous ammonium sulfate were added. The reconstitution was allowed to proceed overnight following which the protein was used for activity measurements. For EcFumA, reconstitution was achieved by the addition of 5 mM DTT for 30 min followed by the addition of 0.5 mM ferrous ammonium sulfate.

### Activity measurements

For recording NMR spectra, the purified recombinant PffH $\Delta$ 40 was incubated with 2, 3-[ $^{13}\text{C}$ ]-fumarate for 30 min at 37 °C in 20 mM sodium phosphate, pH 7.4. The protein was precipitated with TCA and the supernatant, neutralized with 5 N KOH was used for recording  $^{13}\text{C}$ -NMR spectrum in a 400 MHz Agilent NMR machine. D<sub>2</sub>O was added to a final concentration of 10 % to the sample before acquiring the spectrum.

All initial velocity measurements were performed at 37 °C using a spectrophotometric method and initiated with the addition of the enzyme. The activity of EcFumC was measured using a reported method (11) in a solution containing 100 mM MOPS, pH 6.9, 5 mM MgCl<sub>2</sub>, and 5 mM DTT. For EcFumA, the assays were performed in 50 mM potassium phosphate, pH 7.4 containing 2 mM DTT. The activity of PffH $\Delta$ 40 was found to be maximal at pH 8.5 and all assays were carried out at this pH in 50 mM Tris-HCl. The conversion of fumarate to malate was monitored spectrophotometrically as a drop in absorbance caused by the depletion of fumarate. Depending upon the initial concentration of fumarate, the enzymatic conversion was monitored at different wavelengths; 240 nm ( $\epsilon_{240} = 2440 \text{ M}^{-1} \text{ cm}^{-1}$ ) (9) for fumarate concentrations of up to 500  $\mu\text{M}$ , 270 nm ( $\epsilon_{270} = 463 \text{ M}^{-1} \text{ cm}^{-1}$ ) for concentrations ranging from 0.5 to 1.2 mM, 280 nm ( $\epsilon_{280} = 257 \text{ M}^{-1} \text{ cm}^{-1}$ ) for concentrations from 1.2 to 2.6 mM, 290nm ( $\epsilon_{290} = 110 \text{ M}^{-1} \text{ cm}^{-1}$ ) for concentrations from 2.6 to 6 mM, 300 nm ( $\epsilon_{300} = 33 \text{ M}^{-1} \text{ cm}^{-1}$ ) for concentrations from (6 to 20 mM) and 305 nm ( $\epsilon_{305} = 18 \text{ M}^{-1} \text{ cm}^{-1}$ ) for concentrations from (20 to 40 mM) in a quartz cuvette of 1 cm pathlength. The conversion of mesaconate to citramalate was



monitored as drop in absorbance at wavelengths 240 nm ( $\epsilon_{240} = 3791 \text{ M}^{-1} \text{ cm}^{-1}$ ) for concentrations up to 250  $\mu\text{M}$ , 280 nm ( $\epsilon_{280} = 142 \text{ M}^{-1} \text{ cm}^{-1}$ ) for concentrations from 250  $\mu\text{M}$  to 4000  $\mu\text{M}$ , and at 290 nm ( $\epsilon_{290} = 40 \text{ M}^{-1} \text{ cm}^{-1}$ ) for concentrations from 4-16 mM. The use of different wavelengths ensured that the sensitivity of the detection of conversion of fumarate to malate was maximal. The conversion of malate to fumarate was monitored spectrophotometrically as increase in absorbance at 240 nm due to synthesis of fumarate. Activity on tartrate was monitored by a coupled enzyme assay using *P. falciparum* malate dehydrogenase (PfMDH) purified in-house from an *E. coli* expression clone (3). Assay was carried out at 37 °C in 50 mM Tris HCl, pH 8.5 containing 100  $\mu\text{M}$  NADH, 4  $\mu\text{g}$  PfMDH, and 2 mM D-tartrate. The reaction was initiated with 3.4  $\mu\text{g}$  of PFFH.

For testing the effect of small molecules on the activity of PFFH $\Delta$ 40, fumarate was used as the substrate at a concentration of 3 mM. The molecules were tested at a concentration of 0.5 mM. For estimating  $K_i$  values for DL-MSA and meso-tartrate, the initial velocity was measured at varied concentrations of malate (46  $\mu\text{M}$  to 12 mM) / fumarate (24  $\mu\text{M}$  to 25 mM) with DL-MSA/ meso-tartrate fixed at different concentrations. The mode of inhibition was inferred from the type of intersection pattern of lines in the Lineweaver-Burk plot. The  $K_i$  value for DL-MSA was obtained from a global fit of the data by non-linear regression analysis, to a competitive model for enzyme inhibition using GraphPadPrism5.

### **Generation and phenotyping of $\Delta$ fumACB strain of *E. coli***

In order to generate a fumarate hydratase null strain of *E. coli*, a *fumB* null strain (JW4083-1, *fumB748 (del)::kan*) (27), derived from the *E. coli* strain BW25113, was obtained from Coli Genetic Stock Centre (CGSC), Yale university, New Haven, USA (27). To remove the kanamycin cassette flanked by FRT sites at the *fumB* gene locus and to subsequently knockout *fumA* and *fumC*, standard protocols were followed (28) and this is described in **Supplementary Methods** and **Supplementary Figure 1**. Knockout of the genes was validated by PCR using genomic DNA of the mutant strain as template and appropriate oligonucleotides (**Supplementary Table 1**). M9 minimal medium agar plates containing either fumarate or malate (0.4 %) as the sole carbon source and supplemented with trace elements were used to check the phenotype of the strains  $\Delta$ fumACB,  $\Delta$ fumA,  $\Delta$ fumB and  $\Delta$ fumC. Equal number of cells of each of these strains were spread on both malate and fumarate-containing

M9 agar plates and the growth phenotype was scored at the end of 48 h of incubation at 37 °C under aerobic conditions.

### **Complementation of fumarase deficiency in $\Delta$ fumACB strain with PffH and growth inhibition with MSA.**

The  $\Delta$ fumACB strain of *E. coli* was transformed with the plasmids pQE-PffHFL, pQE-PffH $\Delta$ 40, pQE-PffH $\Delta$ 120, and pQE30 and selected on LB plate containing 100  $\mu$ g ml<sup>-1</sup> ampicillin and 50  $\mu$ g ml<sup>-1</sup> kanamycin. A single colony from the plate was inoculated into 10 ml LB broth and allowed to grow overnight. An aliquot of each of the cultures was washed three times with sterile M9 medium to remove traces of LB broth. The cells were resuspended in M9 medium and an OD<sub>600</sub>-normalized aliquot of the suspensions were spread on a M9 agar plate containing the appropriate carbon source and antibiotics. It should be noted that the parent strain BW25113 has a single copy of *lacI*<sup>+</sup> allele and not *lacI*<sup>q</sup> (29) and hence, for induction of protein expression in this strain using pQE30 based constructs, addition of IPTG is optional.

To check the effect of MSA on the *E. coli* strain  $\Delta$ fumACB with the plasmid pQE-PffH $\Delta$ 40, the culture was grown overnight in 10 ml LB medium and 1 ml of the culture was washed twice with M9 minimal medium and resuspended in 1 ml M9 minimal medium. 150  $\mu$ l of this suspension was added to tubes containing 5 ml of M9 minimal medium with 10 mM fumarate as the sole carbon source and appropriate antibiotics (50  $\mu$ g ml<sup>-1</sup> kanamycin and 100  $\mu$ g ml<sup>-1</sup> ampicillin). Varied concentrations of DL-MSA ranging from 1  $\mu$ M to 15 mM were added to the tubes. The growth of the cultures was monitored by measuring OD<sub>600</sub> at the end of 10 h.

### ***P. falciparum* culture, transfection and growth inhibition with MSA**

Intraerythrocytic stages of *P. falciparum* 3D7 strain (procured from MR4) were grown by the method established by Trager and Jensen (30). The parasites were grown in medium containing RPMI-1640 buffered with 25 mM HEPES and supplemented with 20 mM sodium bicarbonate, 0.5 % AlbuMAX I, 0.5 % glucose and 100  $\mu$ M hypoxanthine. O positive erythrocytes from healthy volunteers were added to the culture to a final hematocrit of 2 % for regular maintenance. For examining the localization of PffH, PM1KO strain (26) was transfected with the plasmid pGDB-PffH. For this, pre-loading of erythrocytes (31) with plasmid DNA was carried out by electroporation using a square wave pulse (8 pulses of 365 V each lasting for 1 ms



with a gap of 100 ms) program in BioRad-XL electroporator. Briefly, 100 µg of plasmid DNA dissolved in cytomix (31) was used for transfection of uninfected erythrocytes resuspended in cytomix. After electroporation, the cells were washed with incomplete media to remove cell debris and 1 ml of infected erythrocytes (2 % hematocrit and 6-8 % parasitemia) containing late schizont stage parasites was added. The parasites were allowed to reinvade and when the parasitemia reached 6-8 %, drug selection was started by the addition of trimethoprim (10 µM) and blasticidin S (2.5 µg ml<sup>-1</sup>). The strain of *P. falciparum* is referred to as PfFH-GFP. The strain was subjected to three rounds of drug cycling which included growing the cultures on and off blasticidin (10 days each) in the continuous presence of trimethoprim following which the genotyping of the strain was performed by PCR using genomic DNA as template and primers P1-P4 (**Supplementary Table 1**).

The IC<sub>50</sub> value for DL-MSA for inhibition of parasite growth was determined by a serial two-fold dilution. Briefly, the effect of DL-MSA on the viability of the 3D7 strain of *P. falciparum* was determined by counting the number of parasites in at least 1000 erythrocytes in Giemsa stained smears of cultures grown in the presence of increasing concentrations (3 µM-40 mM) of the drug.

### **Mitochondrial staining and microscopy**

For mitochondrial staining of PfFH-GFP parasites, the culture containing mixed stages of parasites was washed with incomplete medium twice to remove any traces of AlbuMAX I, the cells resuspended with incomplete medium containing 100 nM MitoTracker CM-H<sub>2</sub>XRos and incubated at 37 °C in a candle jar for 30 minutes. For nuclear staining, Hoechst 33342 was added to the culture to a final concentration of 5 µg ml<sup>-1</sup> and incubated for an additional 5 minutes at 37 °C. For imaging, 500 µl of this culture was washed with incomplete medium once and the cells were resuspended in 50 % glycerol/PBS solution. 5 µl of the suspension was placed under a coverslip and imaged using DeltaVision Elite widefield microscope, GE, USA at room temperature. The images were processed using ImageJ (32, 33).

### ***P. berghei* culturing and genetic manipulation**

Intraerythrocytic asexual stages of *P. berghei* ANKA (procured from MR4) were maintained in BALB/c mice. For generation of knockout construct and for transfection of parasites, established procedures were followed (34, 35). Starting from *fh*

genomic library clone (Clone ID: PbG01-2466a09) obtained from PlasmoGEM repository (Wellcome trust Sanger institute, UK), the *fh* gene knockout construct was generated by using the recombineering strategy described by Pfander et al. (32) (**Supplementary Figure 2**). This construct has, flanking the resistance marker, 1395 bp and 2049 bp DNA segments corresponding to regions upstream and downstream, respectively of the *fh* gene to enable gene knockout by double-crossover recombination. For transfection of *P. berghei*, the parasites were harvested from infected mice at a parasitemia of around 1-3 %. Around 0.8-1.0 ml of blood was obtained from each mouse and the parasites were synchronized at schizont stage by *in vitro* growth at 36.5 °C with constant shaking at an optimal speed of 120-150 rpm in medium containing RPMI-1640 with glutamine, 25 mM HEPES, 10 mM NaHCO<sub>3</sub> and 20 % fetal bovine serum under a gassed environment (5 % oxygen, 5 % carbon dioxide and 90 % nitrogen). The schizonts were purified by density gradient centrifugation on Nycodenz and transfected with NotI digested linear DNA of the *fh* gene knockout construct using a 2D-nucleofector (Lonza, Switzerland). Pyrimethamine selection was started 1 day after transfection (35). Limiting dilution cloning of the drug resistant parasites was performed using 16 mice in two batches (32 mice in total). Genomic DNA was isolated from 17 individual parasite lines and subjected to series of diagnostic PCRs to check integration and loss of *fh* gene. The sequences of the oligonucleotides used are provided in Supplementary Table 1.

## RESULTS AND DISCUSSION

### Distribution of Class I fumarate hydratase in eukaryotes

Although both class I and class II FHs catalyze the conversion of fumarate to malate, it is the class II FHs that are widely distributed across eukaryotic organisms. To elicit possible correlations between the presence of class I FH and the nature of the organisms such as their uni- or multi-cellularity and parasitic or free-living lifestyle, eukaryotes with class I FH were catalogued (**Table 1**). In addition, the presence/absence of 1) class II FH in organisms having class I FH and 2) mitochondrial targeting sequence are also included in Table 1. Class I FHs are sparsely distributed in both uni- and multi-cellular eukaryotes and are of the single-subunit type. While most multi-cellular eukaryotes with class I FH also have class II FH, *Hymenolepis microstoma* and *Echinococcus multilocularis* (flatworms) are the

only multicellular eukaryotes that have only class I *fh* gene. Eukaryotes including *Entamoeba histolytica*, *Hymenolepis microstoma*, *Echinococcus granulosus*, *Gonium pectorale*, *Chrysochromulina sp.*, and organisms belonging to Alveolata and Kinetoplastida having only class I FH are all parasitic in nature with the exception of *Chrysochromulina sp.*, and *Gonium pectorale* that are free-living. Most other eukaryotes having class I FH also have the gene for class II FH. *Vitrella brassicaformis*, a photosynthetic ancestor of Apicomplexans (36) has genes for both class I and class II type FH, suggesting the occurrence of a gene loss event with respect to class II FH during the evolution of the Apicomplexan lineage as has been noted previously (20). Of special note are organisms belonging to Kinetoplastida that have two genes for class I FH; one encoding the mitochondrial and other the cytosolic enzyme. Upon search for possible mitochondrial localization of class I and class II FH sequences listed in Table 1 using MitoFates (37), it was seen that in many organisms where both class I and class II FHs are present, class I FH is predicted to localize to mitochondria and not class II FH.

**Table 1. Eukaryotic organisms with class I fumarate hydratase.**

	Organism	Annotation /Accession no. of class I FH	e-value	Life style	Accession no. for class II FH
Alveolata	<i>Perkinsus marinus</i>	FH/ XP_002769256	0.0	[P][U]	A
	<i>Babesia bigemina</i> [ <i>Piroplasma</i> ]	FH/ XP_012767666	0.0	[P] [U]	A
	<i>Theileria annulata</i> [ <i>Piroplasma</i> ]	FH/ XP_954791	0.0	[P] [U]	A
	<i>Plasmodium falciparum</i>	FH/ XP_001352143	0.0	[P] [U]	A
	<i>Toxoplasma gondii</i>	FH/ XP_002368801	0.0	[P] [U]	A
	<i>Cryptosporidium muris</i>	FH/ XP_002140038	0.0	[P] [U]	A
	<i>Neospora caninum</i>	FH/ XP_003880843	0.0	[P] [U]	A
	<i>Hammondia hammondi</i>	FH/ XP_008887656	0.0	[P] [U]	A
	<i>Eimeria tenella</i>	FH/ XP_013233133	0.0	[P] [U]	A
	<i>Symbiodinium microadriaticum</i> [ <i>Dinoflagellates</i> ]	FH/OLQ03181 FH/OLP86388	0.0	[Sy][U]	A
	<i>Vitrella brassicaformis</i> [ <i>chromerida</i> ]	UP/ CEM21256	0.0	[FL] [U]	CEM02426.1
	<i>Chromera velia</i> [ <i>chromerida</i> ]	FH/Cvel_104	0.0	[FL][U]	P(38)
	<i>Cyclospora cayetanensis</i>	FH/ OEH75664.1	0.0	[P][U]	A
Kinetoplastida	<i>Leishmania major</i>	FH/XP_001683549 FH/XP_003722278	0.0 0.0	[P] [U]	A
	<i>Trypanosoma cruzi</i>	FH/XP_817100 FH/XP_814517	0.0 0.0	[P] [U]	A
	<i>Leptomonas pyrrocoris</i>	FH/XP_015657470 FH/ XP_015659024	0.0 0.0	[P] [U]	A
	<i>Phytomonas sp.</i>	UP/CCW59699 UP/ CCW62481	0.0 0.0	[P] [U]	A
	<i>Strigomonas culicis</i>	FH/EPY25531 FH/EPY34169 FH/EPY25825	0.0 0.0 0.0	[P] [U]	A
	<i>Bodo saltans</i>	FH/ CUE71425	3e-116	[P] [U]	A

	<i>Angomonas deanei</i>	HP/EPY26539.1 HP/EPY38000.1 HP/EPY41213.1	6e-96 1e-125 1e-142	[P] [U]	A
Green algae	<i>Volvox carteri f. nagariensis</i>	FH/XP_002956431	0.0	[FL] [M]	XP_002952148.1
	<i>Chlamydomonas reinhardtii</i>	FH/XP_001696634	0.0	[FL] [U]	XP_001689951.1
	<i>Bathycoccus prasinos</i>	FH/XP_007514405	0.0	[FL] [U]	XP_007510319.1
	<i>Gonium pectorale</i>	HP/KXZ553026	0.0	[FL] [U]	A
	<i>Ostreococcus lucimarinus</i>	FH/XP_003078640	0.0	[FL] [U]	XP_001420117.1 XP_001422244.1
Diatom	<i>Micromonas commoda</i>	FH/XP_002501905	0.0	[FL] [U]	XP_002503527.1
	<i>Phaeodactylum tricornutum</i>	FH/XP_002179239	0.0	[FL] [U]	XP_002180479.1
	<i>Thalassiosira pseudonana</i>	FH/XP_002289528	0.0	[FL] [U]	XP_002292587.1
Flat worms	<i>Fragilariopsis cylindrus</i>	FH/OEU13833	0.0	[FL] [U]	OEU16453.1
	<i>Hymenolepis microstoma</i>	FH/CDS31600	0.0	[P][M]	A
	<i>Echinococcus multilocularis</i>	FH/CDI98697	0.0	[P] [M]	A
	<i>Schistosoma mansoni</i>	PR/XP_018648466	0.0	[P] [M]	XP_018645263.1
	<i>Clonorchis sinensis</i>	FH/GAA32985	0.0	[P] [M]	GAA36885.2
	<i>Opisthorchis viverrini</i>	HP/XP_009168721	0.0	[P] [M]	XP_009170493.1
Gastropod	<i>Aplysia californica [California sea hare]</i>	UP/XP_12940821	0.0	[FL] [M]	XP_005106113.1
	<i>Lottia gigantea [Owl limpet]</i>	HP/XP_009058873	0.0	[FL] [M]	XP_009046553.1
	<i>Biomphalaria glabrata</i>	FH/XP_013081380	0.0	[FL] [M]	XP_013069658.1 XP_013069657.1
	<i>Trichuris trichiura [Nematods]</i>	FH/CDW56990	0.0	[FL/P][M]	CDW52898.1
	<i>Helobdella robusta [Segmented worms]</i>	HP/XP_009028259	0.0	[FL] [M]	XP_009019568.1
	<i>Capitella teleta [Segmented worms]</i>	HP/ELT88058	0.0	[FL] [M]	ELT98850.1
	<i>Plutella xylostella [Moths]</i>	UP/XP_011567445	0.0	[FL] [M]	XP_011548738.1 XP_011567303.1
	<i>Trichoplax adhaerens [Lacozoa]</i>	HP/XP_002113462	0.0	[FL] [M]	XP_002117225.1
	<i>Crassostrea gigas (Pacific oyster) [bivalves]</i>	FH/XP_011419283	0.0	[FL] [M]	XP_011416619.1 EKC39898.1
	<i>Octopus bimaculoides [Cephalopods]</i>	HP/KOF97915	0.0	[FL] [M]	XP_014786187.1 XP_014786186.1
	<i>Monosiga brevicollis [Choanoflagellates]</i>	HP/XP_001745789	0.0	[FL] [M]	XP_001747632.1
	<i>Salpingoeca rosetta [Choanoflagellates]</i>	FH/XP_004991224	0.0	[FL] [M]	XP_004993371.1
	<i>Strongylocentrotus purpuratus [Sea urchins]</i>	UP/XP_782370	0.0	[FL] [M]	XP_011675214.1
	<i>Ectocarpus siliculosus [Brown algae]</i>	FH/CBJ30095	0.0	[FL] [M]	CBN75550.1
	<i>Priapululus caudatus [Priapulids]</i>	FH/XP_014672575	0.0	[FL] [M]	XP_014663946.1
	<i>Acanthamoeba castellanii str. Neff [Amoeba]</i>	FH/XP_004336044	0.0	[FL/P][M]	XP_004336877.1
	<i>Branchiostoma floridae [Lancelets]</i>	HP/XP_002613780	0.0	[FL] [M]	XP_002610139.1
	<i>Saccoglossus kowalevskii [Hemichordata]</i>	UP/XP_006819722	0.0	[FL] [M]	XP_002740772.2
	<i>Nannochloropsis gaditana [Algae]</i>	FH/EWM30255	0.0	[FL] [U]	EWM26364.1
	<i>Sphaeroforma arctica [Opisthokont]</i>	FH/XP_014156242	0.0	[FL] [U]	XP_014159970.1
	<i>Entamoeba histolytica [Amoebozoa]</i>	FH/XP_001913833	0.0	[P][U]	A
	<i>Emiliania huxleyi [Haptophytes]</i>	FH/XP_005760439	0.0	[FL] [U]	XP_005760438.1
	<i>Chrysochromulina sp. [Haptophytes]</i>	FH/KOO53837	0.0	[FL] [U]	A
	<i>Blastocystis hominis [Stramenophiles]</i>	UP/XP_012899223 UP/XP_012899254	0.0	[P] [U]	Am
	<i>Aureococcus anophagefferens [Pelagophytes, Stramenophiles]</i>	HP/XP_009035148	0.0	[FL] [U]	XP_009032276.1 XP_009033501.1

<i>Capsaspora owczarzakii</i> [Opisthokont]	FH/XP_004345167	0.0	[Sy][U]	XP_011270881.1
<i>Thecamonas trahens</i>	FH/XP_009058873	0.0	[FL] [U]	XP_013755897.1
<i>Beauveria bassiana</i> [Ascomycetes]	FH/ KGQ13153 FH/ KGQ11123	0.0	[P] [U]	KGQ13152.1 KGQ02326.1 KGQ09969.1
<i>Guillardia theta</i> [Cryptomonad]	HP/XP_005839918	0.0	[FL] [U]	Am
<i>Naegleria gruberi</i> [Percolozoa]	FH/ XP_002683156	0.0	[FL] [U]	XP_002670960.1

FH, fumarate hydratase; HP, hypothetical protein; UP, unknown protein; PR, pol related; [P], parasitic; [FL], free living; [Sy], symbiont; [U], unicellular; [M], multicellular P, present; A, absent; Am, ambiguous. The common names of the organisms are given in square brackets following the Latin names. The list of organisms was obtained from the output of BLASTP using *E. coli* class I FH protein sequence as the query. An e-value cut-off of  $10^{-10}$  and query coverage of 65% were used as criteria for selecting the protein sequences from different organisms. The name of the taxon to which the organism belongs is indicated in some cases in the first column. The *E. coli* FumC protein sequence was used as the query to ascertain the presence or absence of class II fumarate hydratase in these organisms and if present, the accession number of the protein is given in column 6. Ambiguity in the presence of class II FH in some cases is due to the annotation of these proteins as adenylosuccinate lyase with which class II FHs share high sequence similarity. Proteins that are predicted to be localized in the mitochondria are shaded in grey.

### Mitochondrial localization of *P. falciparum* FH

FH in eukaryotes is known to be localized to mitochondria. Though biochemical evidence suggests that FH is mitochondrially localized in *P. falciparum* (3), microscopic images showing localization to this organelle are not available. To examine the localisation of the protein in *P. falciparum*, the *fh* gene on chromosome 9 was replaced with DNA encoding FH-RFA (Fumarate hydratase–regulatable fluorescent affinity tag that comprises GFP, EcDHFR degradation domain and a haemagglutinin tag in tandem) fusion protein by single crossover recombination in PM1KO strain of the parasite (**Figure 1a**). The genotype of the strain (**Figure 1b**) was validated by PCR using primers P1-P4 (**Supplementary Table 1**) and used for live-cell imaging after staining with DAPI and MitoTracker Red CM-H<sub>2</sub>XRos. The GFP-positive parasites clearly showed co-localization of GFP signal with MitoTracker staining (**Figure 1c**) showing mitochondrial localisation of fumarate hydratase in *P. falciparum*.

In order to predict the mitochondrial targeting signal in FH sequences from different *Plasmodium* species, different algorithms were used and the results are summarized in **Supplementary table 2**. Except for *P. knowlesi* FH, wherein all the softwares were able to predict the signal sequence, none of the FH sequences from other *Plasmodium* species had a conventional targeting signal that could be unambiguously predicted. Of all the mitochondrial proteins predicted by PlasMIT, an artificial neural network based prediction tool developed specifically for predicting



mitochondrial transit peptides in *P. falciparum* protein sequences, fumarate hydratase was the only 'false negative' (39). This suggests that PfFH localization to the mitochondrion is possibly mediated through an internal signal sequence or an unconventional mitochondrial localization signal.

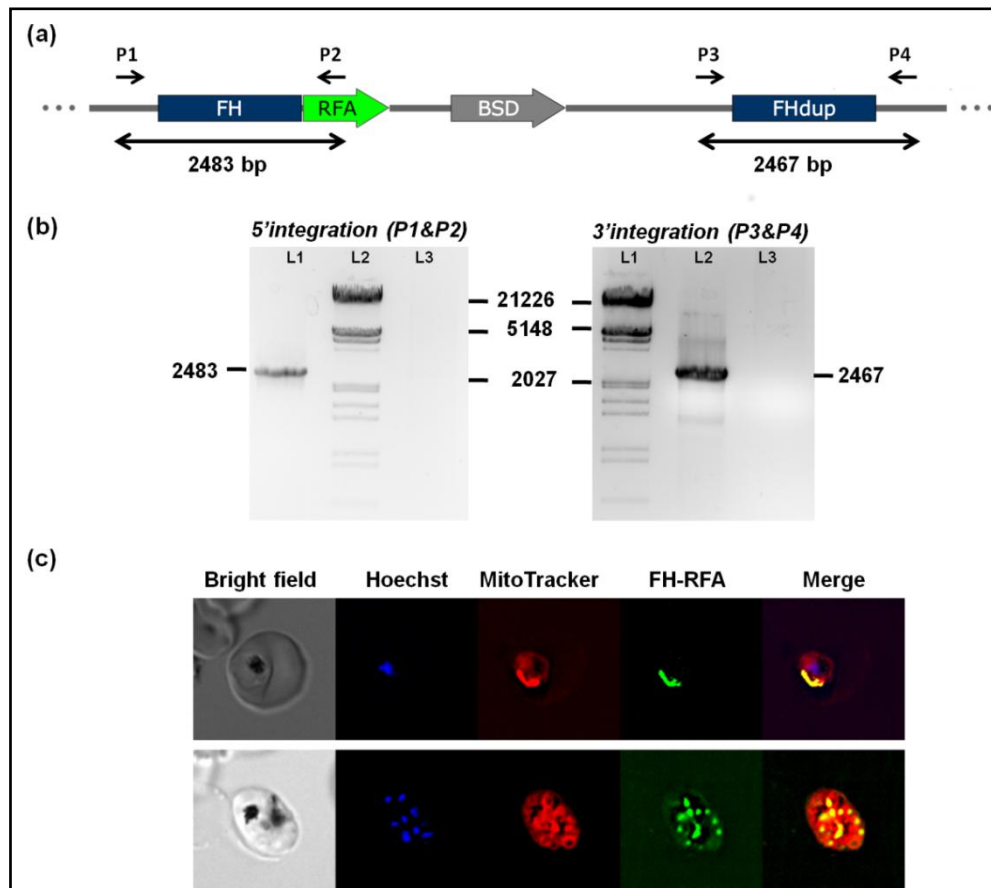


**Figure 1. Generation of PfFH-GFP strain encoding FH-GFP and localisation of PfFH.** (a) Scheme showing the integration locus with the RFA (GFP+DHFRdd+HA)-tag in tandem with FH gene in the strain PfFH-GFP. Oligonucleotides P1 and P2 and, P3 and P4 were used for checking the 5'- and 3'- integration, respectively (**Supplementary Table 1**). P1 and P4 are beyond the sites of integration in the genome. (b) Left panel, genotyping by PCR for validating 5' integration. The templates used in different lanes are, L1, genomic DNA from PfFH-GFP, L3, *P. falciparum* PM1KO genomic DNA. A band of size 2483 bp validates 5' integration. Right panel, genotyping by PCR for validating 3' integration. The templates used in different lanes are, L2, genomic DNA from PfFH-GFP, L3, *P. falciparum* PM1KO genomic DNA. A band of size 2467 bp validates 3' integration. Molecular weight markers are in lanes L2 and L1 in right and left panels, respectively. (c) Upper panel shows a trophozoite and the lower panel, a schizont. As evident from the merge PfFH localizes to the mitochondrion.



### **PfFH complements fumarase deficiency in *E. coli***

In order to recombinantly express organellar proteins in *E. coli*, it is preferable to use the DNA sequence corresponding to only the mature protein with the signal peptide deleted. Since none of the bioinformatic prediction tools were able to identify an unambiguous signal sequence in *P. falciparum* FH, we resorted to multiple sequence alignment with bacterial single-subunit type and archaeal two-subunit type FH for generating N-terminal deletion constructs. Examination of the multiple sequence alignment shows a 120 amino acid insertion at the N-terminus in *Plasmodium* FHs that is absent in bacterial and archaeal FH sequences (**Supplementary Figure S3**). Of the N-terminal 120 amino acid residues in *Plasmodial* FHs, the first 40 residues are diverse, while residues 40-120 show a high degree of conservation (**Supplementary Figure S4**) within the genus. Hence, for functional complementation in *E. coli fh* null mutant, three different expression constructs of PfFH protein in pQE30 were generated; that expressing the full length (PfFHFL), N-terminal 40 residues deleted (PfFH $\Delta$ 40) and N-terminal 120 residues deleted (PfFH $\Delta$ 120) enzymes.

*E. coli* has three genes that encode fumarate hydratase; *fumA* and *fumB* of the class I type and *fumC* of the class II type. *fumA* and *fumC* genes are in tandem and are driven by a common promoter (7, 40). Starting with JW4083-1, a  $\Delta$ *fumB* strain of *E. coli*, a triple knockout  $\Delta$ *fumACB* strain, in which all the three major *fum* genes (*fumA*, *fumC* and *fumB*) are deleted, was generated and validated by PCR (**Supplementary Figure S1**). As expected, while the strain was able to grow normally in malate containing minimal medium (**Figure 2a**), it was unable to grow on minimal medium containing fumarate as the sole carbon source (**Figure 2b**). As expected all transformants (containing pQE-PfFHFL, pQE-PfFH $\Delta$ 40, pQE-PfFH $\Delta$ 120 and pQE30) of  $\Delta$ *fumACB* strain of *E. coli* grew well on malate containing minimal medium plates (**Figure 2c**). In the fumarate containing M9 plate, the cells expressing PfFH $\Delta$ 40 and PfFHFL grew faster, whereas, the growth rate of cells expressing PfFH $\Delta$ 120 was slower and no growth of cells carrying just pQE30 was observed (**Figure 2d**). This shows that the PfFH can functionally complement the deficiency of fumarate hydratase activity in  $\Delta$ *fumACB* strain and validates that the *P. falciparum* enzyme is indeed fumarate hydratase. The slow growth of PfFH $\Delta$ 120 expressing  $\Delta$ *fumACB* *E. coli* strain indicates that residues 40-120 play a role in the structure and/or function of PfFH despite these residues being conserved only in *Plasmodial*

fumarate hydratase sequences and not in others (**Supplementary Figure S3**).

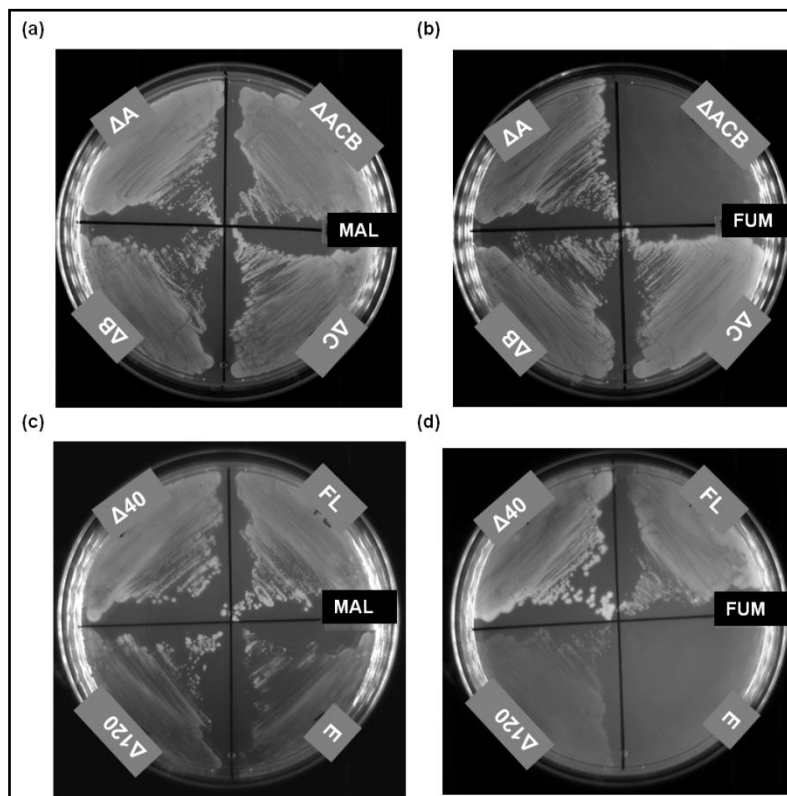


**Figure 2. Phenotyping of the *E. coli* strain  $\Delta$ fumACB and functional complementation by *P. falciparum* FH.** Growth phenotype of the *E. coli* strains with at least one copy of fumarate hydratase gene deleted on **(a)** malate and **(b)** fumarate containing minimal medium. As it is evident from the phenotype,  $\Delta$ fumACB strain is not able to grow on fumarate containing minimal medium. The growth of  $\Delta$ fumACB strains expressing either P<sub>f</sub>FH<sub>FL</sub> or P<sub>f</sub>FH $\Delta$ 40 or P<sub>f</sub>FH $\Delta$ 120 of *P. falciparum* fumarate hydratase on **(c)** malate- and **(d)** fumarate-containing minimal medium. The plates were scored after 48 h of incubation at 37 °C.  $\Delta$ fumACB strain containing just pQE30 (E) was used as a control. The experiment was repeated thrice and the images correspond to one of the replicates.

### Activity of P<sub>f</sub>FH $\Delta$ 40

P<sub>f</sub>FH $\Delta$ 40 was expressed with an N-terminal (His)<sub>6</sub>-tag in Codon plus BL21 (DE3) RIL, purified using Ni-NTA affinity chromatography (**Figure 3a**) and reconstituted *in vitro* with Fe-S cluster. The UV-visible spectrum with absorption maximum at 360 and 405 nm indicates the presence of 4Fe-4S cluster in the enzyme. Addition of sodium dithionite reduced the absorption at 405 nm indicating reduction of the cluster (**Figure 3b**) (41–44). The enzyme lacking the reconstituted cluster was devoid of any activity. The activity of P<sub>f</sub>FH $\Delta$ 40 when examined at 240 nm showed a time

dependent decrease in absorbance with fumarate as the substrate, while with malate an increase was observed. To confirm the chemical identity of the product formed, NMR spectrum was recorded with 2, 3- $^{13}\text{C}$ -fumarate as the substrate. Appearance of two doublets with chemical shift values 70.63, 70.26 ppm and 42.86, 42.29 ppm corresponding to C2, C3 carbons, respectively of malate confirmed that PffH $\Delta$ 40 has *in vitro* fumarase activity (**Figure 3c**).

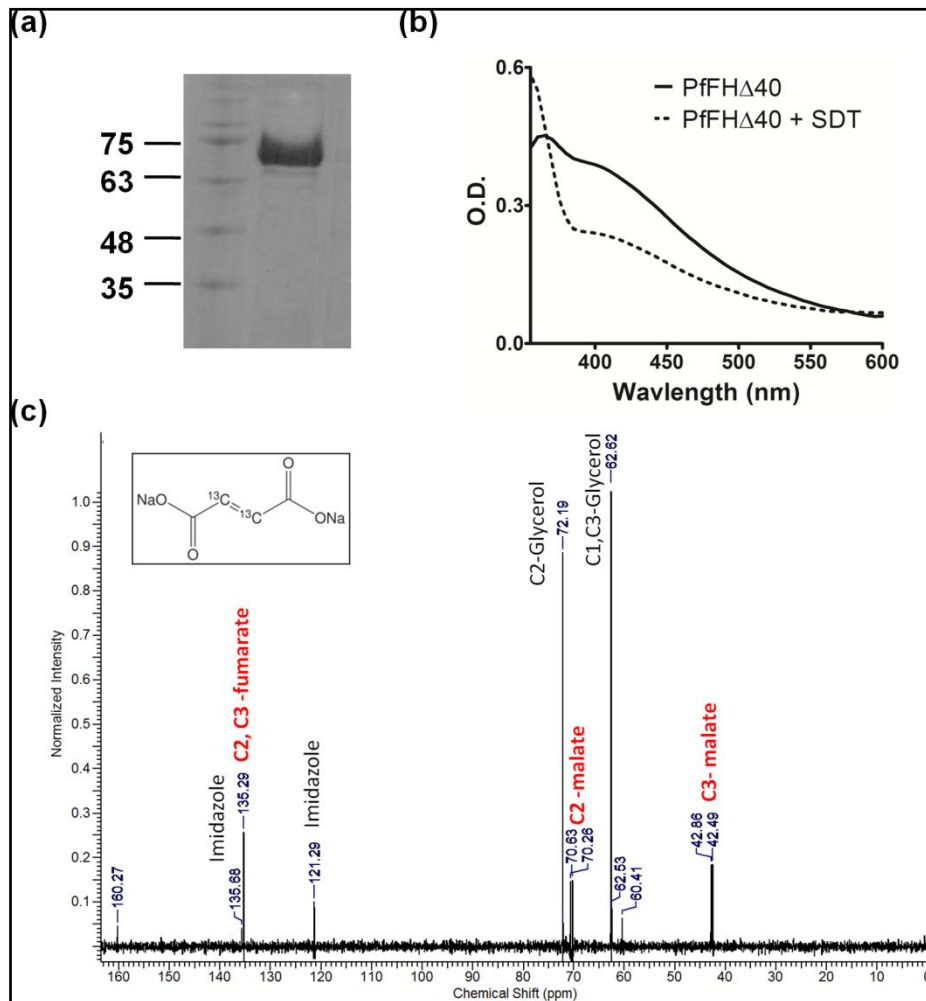


**Figure 3. Purification and activity of PffH $\Delta$ 40.** (a) Lane 1, protein molecular weight marker (numbers indicated are in kDa); lane 2, Ni-NTA purified PffH $\Delta$ 40. (b) UV-visible absorption spectrum of purified and reconstituted PffH shows characteristic peak at 360 and 405 nm that indicates the presence of 4Fe-4S cluster. (c) Validation of malate formation by  $^{13}\text{C}$ -NMR. The NMR spectrum of assay mixture consisting of 50  $\mu\text{M}$  2,3- $^{13}\text{C}$ -fumarate in 100 mM potassium phosphate, pH 7.4, incubated with 100  $\mu\text{g}$  of purified PffH $\Delta$ 40 enzyme, shows the presence of peaks corresponding to  $^{13}\text{C}$ -malate. Unreacted  $^{13}\text{C}$ -fumarate is also

present. The inset shows the chemical structure of  $^{13}\text{C}$ -fumarate. The spectrum is an average of 3000 scans acquired using Bruker 400MHz NMR spectrometer. The peaks corresponding to imidazole and glycerol are from the protein solution.

Substrate saturation curves for PfFH $\Delta$ 40 for both fumarate and malate were hyperbolic in nature indicating the absence of cooperativity. Fit to Michaelis -Menton equation yielded  $K_m$  and  $V_{max}$  values that are summarized in **Table 2**. The  $K_m$  values for PfFH $\Delta$ 40 for fumarate and malate in the low millimolar range are similar to that of class I FH from *Leishmania major* (21) and *Trypanosoma cruzi* (22) while for those from bacteria and archaea, the values are in the micromolar range. The catalytic efficiency ( $k_{cat}/K_m$ ) of PfFH $\Delta$ 40 is similar to *L. major* FH but 10-100 fold lower than that reported for other class I FHs (**Table 2**). The substrate promiscuity of PfFHFL, PfFH $\Delta$ 40, and PfFH $\Delta$ 120 for other dicarboxylic acids was examined using growth complementation in the *E. coli* strain,  $\Delta$ *fumACB* (**Figure 4**). Growth on L-tartrate, D-tartrate, and itaconate were conditional to the presence of PfFH, while growth on meso-tartrate was independent. All three PfFH constructs greatly enhanced the growth of  $\Delta$ *fumACB* strain of *E. coli* on mesaconate over the control. *In vitro* activity measurements showed that the parasite enzyme utilizes mesaconate as a substrate converting it to S-citramalate with  $K_m$  and  $k_{cat}/K_m$  values of  $3.2 \pm 0.3$  mM and  $1.7 \times 10^4 \text{ M}^{-1} \text{ s}^{-1}$ , respectively with the latter value 3.5- and 10-fold lower than that for fumarate and malate, respectively (**Table 2**). The *in vitro* activity on D-tartrate was measured by a coupled enzyme assay using PfMDH. This activity at 2 mM D-tartrate was  $7.8 \mu\text{mole min}^{-1} \text{ mg}^{-1}$  that is 9.4-fold lower than that on malate at similar concentration. The poor growth of  $\Delta$ *fumACB* strain expressing PfFH constructs on this substrate correlates with the weak *in vitro* activity. Inhibition of PfMDH (the coupling enzyme) at higher concentration of D-tartrate precluded estimation of  $k_{cat}$  and  $K_m$  values for this substrate. PfFH $\Delta$ 40 failed to show *in vitro* activity on itaconate (a succinate analog), R-malate and R, R-tartrate (L-tartrate) even at a concentration of 10 mM, indicating that the enzyme is highly stereospecific in recognition of substrates. The growth phenotype of  $\Delta$ *fumACB* on R,R-tartrate and itaconate could arise from PfFH playing a secondary but critical role required for cell growth. These results show that the substrate promiscuity profile of PfFH is similar to class I enzymes from other organisms (7, 9, 14, 45) with the order of preference being fumarate followed by mesaconate and the least preferred being D-tartrate.

**Table 2. Kinetic parameters of PfFH $\Delta$ 40 and other class I FH**

No	Org./Enzyme name	Substrate	$K_m$ (mM)	$V_{max}$ or $k_{cat}$ (#)	$k_{cat}/K_m$	Ref.
1	<b><i>P. falciparum</i></b> <i>PfFH<math>\Delta</math>40</i>	Fumarate	2.6 $\pm$ 0.3	138 $\pm$ 3	6.2 $\times$ 10 <sup>4</sup>	This study
		Malate	1.2 $\pm$ 0.1	127 $\pm$ 4	1.3 $\times$ 10 <sup>5</sup>	
		Mesaconate	3.2 $\pm$ 0.3	48 $\pm$ 2	1.7 $\times$ 10 <sup>4</sup>	
2	<b><i>T. cruzi</i></b> TcFHc	Fumarate	0.8 $\pm$ 0.2*	400 $\pm$ 100 <sup>#</sup>	8.2 $\times$ 10 <sup>6</sup>	(22)
		Malate	2.5 $\pm$ 0.6*	290 $\pm$ 40 <sup>#</sup>	1.3 $\times$ 10 <sup>6</sup>	
		TcFHm	Fumarate	1.5 $\pm$ 0.4	2300+500 <sup>#</sup>	
		Malate	2.8 $\pm$ 0.2	1050 $\pm$ 40 <sup>#</sup>	0.4 $\times$ 10 <sup>6</sup>	
3	<b><i>E. coli</i></b> <i>Fum A</i>	Fumarate	0.09 $\pm$ 0.02	614 $\pm$ 29	6.6 $\times$ 10 <sup>6</sup>	(14)
		Malate	0.40 $\pm$ 0.05	350 $\pm$ 10	8.7 $\times$ 10 <sup>6</sup>	
		Mesaconate	0.22 $\pm$ 0.02	55.6 $\pm$ 1.7	2.5 $\times$ 10 <sup>6</sup>	
	<i>Fum B</i>	Fumarate	0.21 $\pm$ 0.03	654 $\pm$ 38	3.1 $\times$ 10 <sup>6</sup>	
		Malate	0.78 $\pm$ 0.13	289 $\pm$ 16	3.7 $\times$ 10 <sup>6</sup>	
		Mesaconate	0.10 $\pm$ 0.01	57.8 $\pm$ 1.4	5.8 $\times$ 10 <sup>5</sup>	
4	<b><i>L. major</i></b> <i>LMFH-1</i>	Fumarate	2.5 $\pm$ 0.4	26.4 $\pm$ 4.4	1.1 $\times$ 10 <sup>4</sup>	(21)
		Malate	2.3 $\pm$ 0.3	11.8 $\pm$ 1.2	5.6 $\times$ 10 <sup>3</sup>	
	<i>LMFH-2</i>	Fumarate	5.7 $\pm$ 1.4	186 $\pm$ 46.5	3.6 $\times$ 10 <sup>4</sup>	
		Malate	12.6 $\pm$ 2.7	138 $\pm$ 18.7	1.2 $\times$ 10 <sup>4</sup>	
5	<b><i>P. furiosus</i></b> <i>FH</i>	Fumarate	0.34	1376	3.2 $\times$ 10 <sup>6</sup>	(46)
		Malate	0.41	1892	3.7 $\times$ 10 <sup>6</sup>	
6	<b><i>P. thermop.</i></b> <i>MmcBC</i>	Fumarate	0.43	219 <sup>#</sup>	5.1 $\times$ 10 <sup>5</sup>	(8)
		Malate	0.59	25.2 <sup>#</sup>	4.3 $\times$ 10 <sup>4</sup>	
7	<b><i>B. xerov.</i></b> <i>Bxe_A3136</i>	Fumarate	0.10 $\pm$ 0.01	296 $\pm$ 5	2.8 $\times$ 10 <sup>6</sup>	(10)
		Malate	0.28 $\pm$ 0.02	118 $\pm$ 3	3.98 $\times$ 10 <sup>5</sup>	
		Mesaconate	0.03 $\pm$ 0.01	117 $\pm$ 6	3.6 $\times$ 10 <sup>6</sup>	

The units for  $V_{max}$ ,  $k_{cat}$  and  $k_{cat}/K_m$  are  $\mu\text{mole min}^{-1}\text{mg}^{-1}$ ,  $\text{s}^{-1}$  and  $\text{s}^{-1}\text{M}^{-1}$ , respectively.



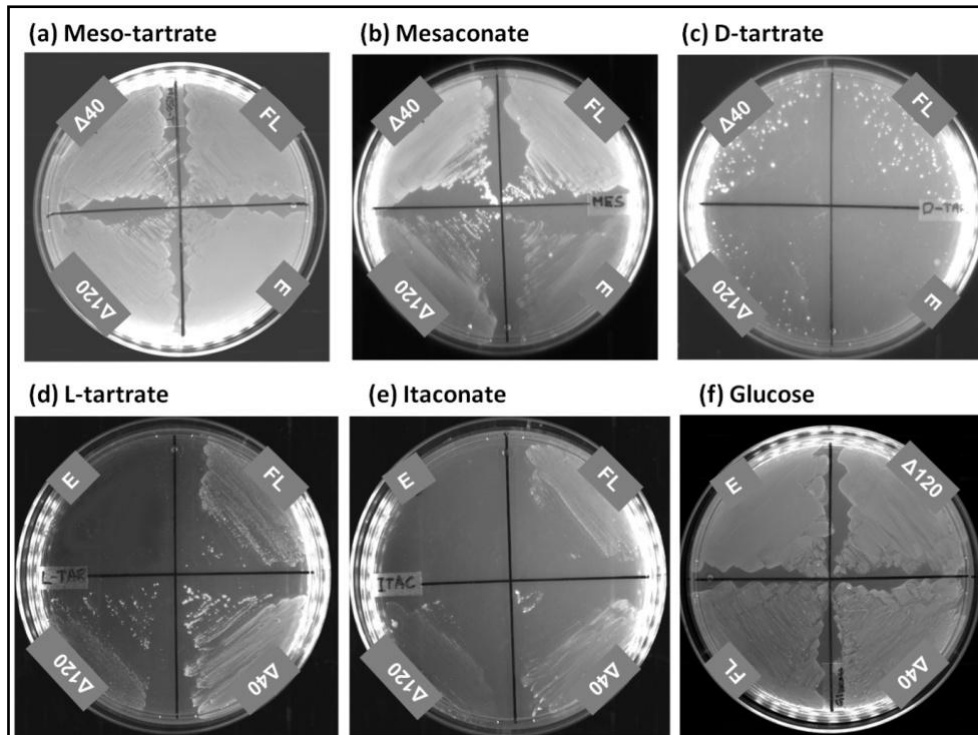


**Figure 4. Growth of *E.coli* strain  $\Delta$ *fumACB* expressing PfFH on different carbon sources.** The growth of  $\Delta$ *fumACB* strains expressing either PfFH<sub>FL</sub> or PfFH $\Delta$ 40 or PfFH $\Delta$ 120 were tested on (a) meso-tartrate, (b) mesaconate, (c) D-tartrate, (d) L-tartrate, (e) itaconate and (f) glucose - containing minimal medium. The plates were scored after 48 h of incubation at 37 °C.  $\Delta$ *fumACB* strain containing just pQE30 (E) was used as a control. The experiment was repeated thrice and the images correspond to one of the replicates. The glucose containing plate served as control for the number of cells plated across the different constructs.

### **Mercaptosuccinic acid is class I FH specific inhibitor**

Analogs of fumarate, malate, and intermediates of the TCA cycle (including their analogs) were tested for their effect on PfFH $\Delta$ 40 (Supplementary methods). Of these, the only molecules that inhibited PfFH activity were DL-mercaptosuccinic acid (DL-MSA, **Figure 5 a**) and meso-tartrate. Double reciprocal plots of initial velocity as a function of varied substrate (fumarate and malate) concentrations at different fixed DL-MSA concentrations yielded lines that intersected on the 1/v axis indicating the competitive nature of inhibition (**Figure 5b and 5c**). The  $K_i$  values for DL-MSA for PfFH $\Delta$ 40 with malate and fumarate as substrates are  $321 \pm 26$  nM and  $548 \pm 46$  nM, respectively. To test the specificity of MSA for class I FH, its effect on both EcFumA and EcFumC were examined. The  $K_i$  value for the inhibition of EcFumA with



fumarate as the substrate was  $2.9 \pm 0.22 \mu\text{M}$  indicating that DL-MSA is 5.2-fold more potent for P<sub>f</sub>FH $\Delta$ 40. It should be noted that the MSA used in the studies is an enantiomeric mixture of DL-isomers and hence, the  $K_i$  value would be half of that determined. Further, as D-malate is not an inhibitor of P<sub>f</sub>FH, only L-MSA would be expected to bind to the enzyme. DL-MSA was also found to inhibit the two-subunit class I FH from *Methanocaldococcus jannaschii* (unpublished) while, there was no effect on EcFumC even at a concentration of 10 mM indicating its exclusive specificity for class I FH. A recent study has reported the inhibition of TcFH by DL-MSA with a  $K_i$  of  $4.2 \pm 0.5 \mu\text{M}$  while no effect was observed on the class II human FH (22). Interestingly, DL-MSA is not a substrate for P<sub>f</sub>FH as seen by spectrophotometric assays at 240 nm with 10 mM DL-MSA and 1  $\mu\text{M}$  enzyme that failed to show either formation of the enediolate intermediate or the product fumarate through liberation of H<sub>2</sub>S. The reason for DL-MSA's high specificity for class I FH must stem from the presence of 4Fe-4S cluster that interacts with the C2-hydroxyl group of malate (11). Replacement of the hydroxyl group with a thiol probably leads to tight binding through Fe-S interaction. Also, the formation of a stable DL-MSA-FH complex could arise from the C3-hydrogen of DL-MSA being less acidic than that of malate. The 4Fe-4S cluster containing quinolinate synthase (NadA) is strongly inhibited by dithiohydroxyphthalic acid (DTHPA), the thio-analog of the transition state intermediate of the reaction catalyzed, in a manner similar to MSA inhibition of class I FH. Interactions of the thiol groups of DTHPA with Fe atom of the cluster leads to strong binding affinity for the enzyme (47). In this context we expect thio-mesaconate and S,S-dithiotartrate, analogs of the substrates mesaconate and S,S, tartrate (D-tartrate) to be also strong inhibitors of class I FH.

Albeit slightly less effective as an inhibitor, meso-tartrate competitively inhibited P<sub>f</sub>FH $\Delta$ 40 with a  $K_i$  value of  $114 \pm 17 \mu\text{M}$ . This compound inhibited both EcFumA and EcFumC with similar  $K_i$  values of 625 and 652  $\mu\text{M}$ , respectively. Meso-tartrate has two chiral carbons with S- configuration at C2, and R- configuration in C3. It should be noted that in the case of both EcFumC and EcFumA S,S-tartrate (D-tartrate) is a substrate (14). The inhibition by meso-tartrate of both class I and II FH indicates relaxed stereospecificity of these enzymes at the C3 carbon of the substrates. Pyromellitic acid, a known potent inhibitor of class II FH had no effect on the activity of the two class I enzymes tested (P<sub>f</sub>FH $\Delta$ 40 and EcFumA), while completely abolishing the activity of the class II enzyme (EcFumC). The specificity

exhibited by DL-MSA for class I FH and, pyromellitic acid and S-2,3-dicarboxyaziridine (48) for class II FH supports the presence of different active site environments in the two classes of enzymes. This provides a framework for developing class I PfFH (and in general for class I FH) specific inhibitors that will have no effect on the human enzyme.

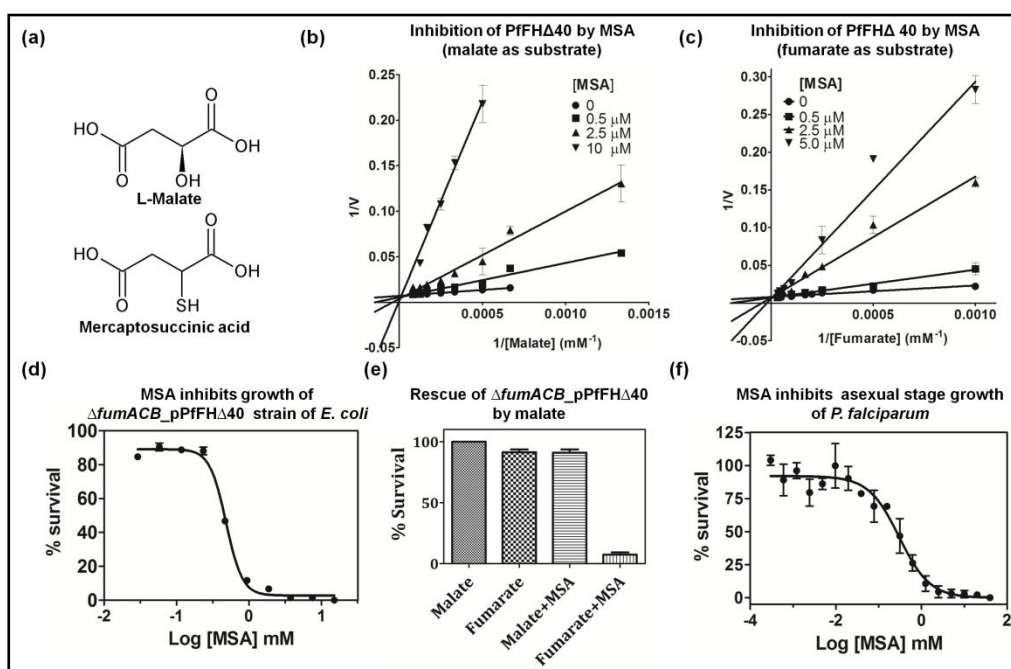


**Figure 5. Specificity of DL-MSA for class I FH.** (a) Structures of L-malate and mercaptosuccinic acid. (b) Lineweaver-Burk plot of initial velocity at varied malate and different fixed MSA concentrations. (c) Lineweaver-Burk plot of the initial velocity at varied fumarate and different fixed MSA concentrations. (d) Inhibition of the growth of  $\Delta fumACB\_pPfFH\Delta 40$  strain of *E. coli* by MSA. (e) Rescue of MSA mediated growth inhibition of  $\Delta fumACB\_pPfFH\Delta 40$  upon addition of malate. (f) Inhibition of the in vitro growth of intraerythrocytic asexual stages of *P. falciparum* by MSA.

### Growth inhibition by DL-MSA

Since the growth of *E. coli*  $\Delta fumACB$  strain on minimal medium containing fumarate as the sole carbon source is conditional to the presence of functional FH, the effect of DL-MSA on the growth of  $\Delta fumACB\_pPfFH\Delta 40$  was examined. DL-MSA inhibited the growth of  $\Delta fumACB\_pPfFH\Delta 40$  with an  $IC_{50}$  of  $482 \pm 4 \mu M$  (Figure 5d) and addition of malate completely rescued the inhibition (Figure 5e). This shows that the toxicity of DL-MSA is indeed due to inhibition of the metabolic conversion of fumarate to malate.  $\Delta fumACB$  *E. coli* strain can serve as a facile primary screening system for

small molecules acting as inhibitors of PfFH as it circumvents *in vitro* assays with the oxygen-sensitive labile enzyme. With DL-MSA as an inhibitor of PfFH under *in vitro* and *in vivo* conditions, the molecule was checked for its toxicity on intra-erythrocytic stages of *P. falciparum* in *in vitro* culture. DL-MSA was found to kill parasites in culture with an IC<sub>50</sub> value of 281 ± 68 µM (**Figure 5f**). Though DL-MSA is a potent inhibitor of PfFHΔ40 with a K<sub>i</sub> value of 547 ± 47 nM (with fumarate as substrate), the IC<sub>50</sub> values for the inhibition of both Δ*fumACB*\_pPfFHΔ40 and *P. falciparum* are significantly higher.

### **Fumarate hydratase is essential for *Plasmodium berghei***

Earlier attempt at knockout of fumarate hydratase gene in *P. falciparum* was not successful (23). Therefore, the essentiality of FH was examined in *P. berghei* with BALB/c mice as host. For this, *fh* gene knockout construct generated through recombineering based strategy was used (**Supplementary Figure S2**). Transfected parasites were injected into mice, selected on pyrimethamine and drug resistant parasites that appeared 10 days after infection were subjected to limiting dilution cloning. All the 17 *P. berghei* clones (A to Q) obtained by limited dilution cloning of the drug resistant parasites were examined by PCR to confirm the presence of the integration cassette and the absence of the *fh* gene. Oligonucleotides used for genotyping of the clones are provided in **Supplementary Table 1**. The expected genomic locus upon integration of selectable marker cassette by double crossover recombination is shown schematically in **Figure 6 a** and the wild-type (with *fh* gene) is shown in **Figure 6 b**. Genotyping by PCR was performed to confirm integration of selectable marker cassette at expected locus (**Figure 6 d & e**), presence/absence of the *fh* gene (**Figure 6 f**) and the presence of the selection cassette (**Figure 6 g & h**). The results of the PCRs showed that though all the parasite clones carried the selectable marker, hDHFR-yFCU cassette in the genomic DNA (**Figure 6 g**), they also retained the *fh* gene (**Figure 6 f**). In two of the clones (C and O), the integration of the cassette was at a random site as they failed to answer for both 5' and 3' integration PCRs. 12 clones yielded the expected PCR amplified fragment for 5' integration (**Figure 6 d**) while a band of the expected size was not obtained for 3' integration PCR. One clone (M) yielded expected PCR amplified fragment for only 3' integration (**Figure 6 e**) and not for 5' integration. Integration of the selection cassette through single crossover recombination using 5' or 3' homology arm with

the intact *fh* gene present downstream or upstream, respectively would yield this PCR result. As the DNA used for transfection was linear, circularization of the fragment must have enabled this single crossover recombination. Only 2 clones (J and Q) answered positive for both 5' and 3' integration PCRs, while continuing to harbor the *fh* gene. These two clones must have arisen from a double crossover recombination event in a population of parasites harboring the duplicated copy of the *fh* gene. Although parasites with gene duplication are thought to be unstable, existence of duplication has been noted earlier in the case of *rio2* (49) and *dhodh* (50). The variation in the genotype across the 17 clones that we have obtained shows that the parasites have not multiplied from a single wrong event of homologous recombination. On the contrary, the presence of clonal population with different genotypes suggests a strong selection pressure for the retention of *fh* gene.

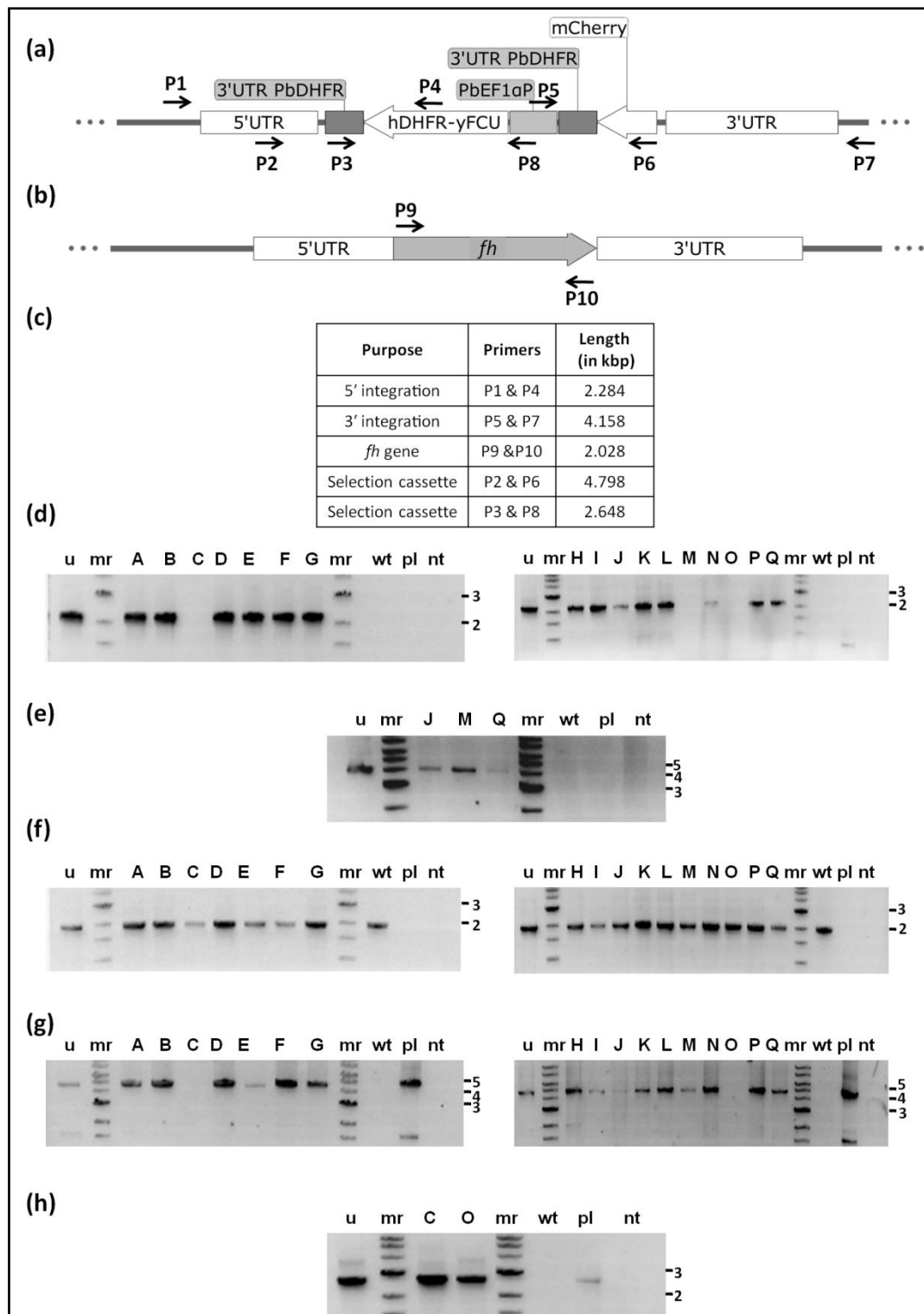


**Figure 6. Genotyping of *P. berghei* clones of knockout of fumarate hydratase.** (a) Schematic representation of the selectable marker cassette inserted into the *fh* gene locus of *P. berghei* genome. Primers (P1-P8) used for diagnostic PCRs are indicated. (b) Schematic representation of the *fh* gene (PBANKA\_0828100) flanked by 5' UTR and 3' UTR showing the location of primers P9 and P10. (c) Table showing the combination of primers used, size of the expected product and the diagnostic purpose. PCR of (d) clones A-G (left panel) and (e) clones H-Q (right panel) and (f) clones A-G (left panel) and (g) clones H-Q (right panel) and (h) clones C and O.

clones H-Q (right panel) for detection of 5' integration; (e) clones J, M and Q for detection of 3' integration (other clones did not answer for this PCR); (f) clones A-G (left panel) and clones H-Q (right panel) for the detection of *fh* gene; (g) clones A-G (left panel) and H-Q (right panel) for the presence of selectable marker cassette; (h) clones C and O using primers P3 and P8. Clones C, M and O did not answer for 5' integration while only clones J, M and Q answered for 3' integration. All clones answered for the presence of the *fh* gene (Panel e). All clones except C and O answered by PCR with primers P2 and P6 indicating the integration of the entire selectable marker cassette into the genome. Clones C and O answered for a shorter fragment of the selectable marker cassette covered by primers P3 and P8. *hDHFR-yFCU*, human DHFR-yeast cytosine and uridyl phosphoribosyltransferase, *u*, uncloned population, *mr*, molecular weight marker; *wt*, wild-type *P. berghei* genomic DNA; *pl*, *pJAZZ-FH* knockout construct (supplementary figure S2); *nt*, control PCR without template. Numbers to the right of panels d, e, f, g and h are the sizes of the marker DNA fragments in kbp.

The PCRs with primers P9 and P10 (**Figure 6 f**) encompassing the full length gene yielded the expected size band with genomic DNA from all 17 clones, indicating that all clones contain full length *fh* gene. A study that appeared recently reports on the knockout of *fh* gene in *P. berghei*, with the knockout parasites exhibiting slow growth phenotype (51). Though the authors show absence of *fh* gene expression in the knockout strain, the genotyping for confirmation of knockout that was carried out with oligonucleotide primers corresponding to the homology arm used for recombination cannot confirm the site of integration. Apart from the length of the homology arm used for recombination, the key difference is with regard to the strains of mice used. While, our study has used BALB/c, Niikura et al, (51) have used C57 strain of mice. *P. berghei* is known to exhibit differences in growth and infectivity across different strains of mice. Our inability to obtain a knockout of *fh* could also suggest host strain specific essentiality of the parasite *fh* gene. It should be noted that Ke et al, 2015 (23) have also reported the inability to knockout *fh* in *P. falciparum*.

## CONCLUSION

Unlike higher eukaryotes including humans that have only class II fumarate hydratase, most parasitic protozoa have only the class I enzyme. The class I FH in *P. falciparum* localizes only to the mitochondrion, though a mitochondrial targeting



signal sequence could not be identified using any of the bioinformatic tools. Upon expression as recombinant proteins in *E. coli*, of the three constructs, PfFHFL, PfFH $\Delta$ 40, and PfFH $\Delta$ 120, the highest level of soluble protein was obtained with PfFH $\Delta$ 40. The purified, Fe-S cluster-reconstituted PfFH $\Delta$ 40 was active and catalyzed the reversible conversion of fumarate and malate with a lower  $K_m$  value for malate and similar  $k_{cat}$  values for both the forward and reverse reactions. The parasite enzyme complements fumarase deficiency in *E. coli*. Both *in vitro* and *in vivo* in *E. coli*, PfFH exhibits extended substrate specificity for D-tartrate and mesaconate. The significance of the extended substrate specificity of PfFH for mesaconate and D-tartrate with regard to *Plasmodium* cellular biochemistry is unclear at this stage.

MSA is a highly potent and specific inhibitor of class I FH *in vitro*. Surprisingly, *in vivo*, in both *E. coli* expressing PfFH and intraerythrocytic *P. falciparum*, the IC<sub>50</sub> values for cell death are significantly higher (in the micromolar range). The rescue of the growth inhibition of the *E. coli* cells by malate indicates that the inhibitory effect *in vivo* is specifically through PfFH. The discrepancy between the  $K_i$  value for the purified enzyme and the IC<sub>50</sub> value on cells could be either due to low intracellular availability of the drug (owing to the hydrophilic nature of the molecule and hence poor transport) or due to metabolism leading to degradation of MSA. MSA dioxygenase, an enzyme that converts mercaptosuccinic acid to succinate is present in the bacterium *Variovorax paradoxus* (52, 53). We however, could not find homologues of the enzyme in *E. coli* or *P. falciparum*. In addition, in *P. falciparum*, the host erythrocyte in which the parasite resides contains the class II enzyme that is not inhibited by MSA and this could substitute for the lack of parasite FH activity. However, under these conditions, regeneration of aspartate (3) and NAD<sup>+</sup> pools from fumarate mediated by PfFH would require the transport of intermediates across the 3 compartments (erythrocyte, parasite and the mitochondrion), evidence for which is absent. Therefore, the effectiveness of substitution of PfFH by the human enzyme is unclear.

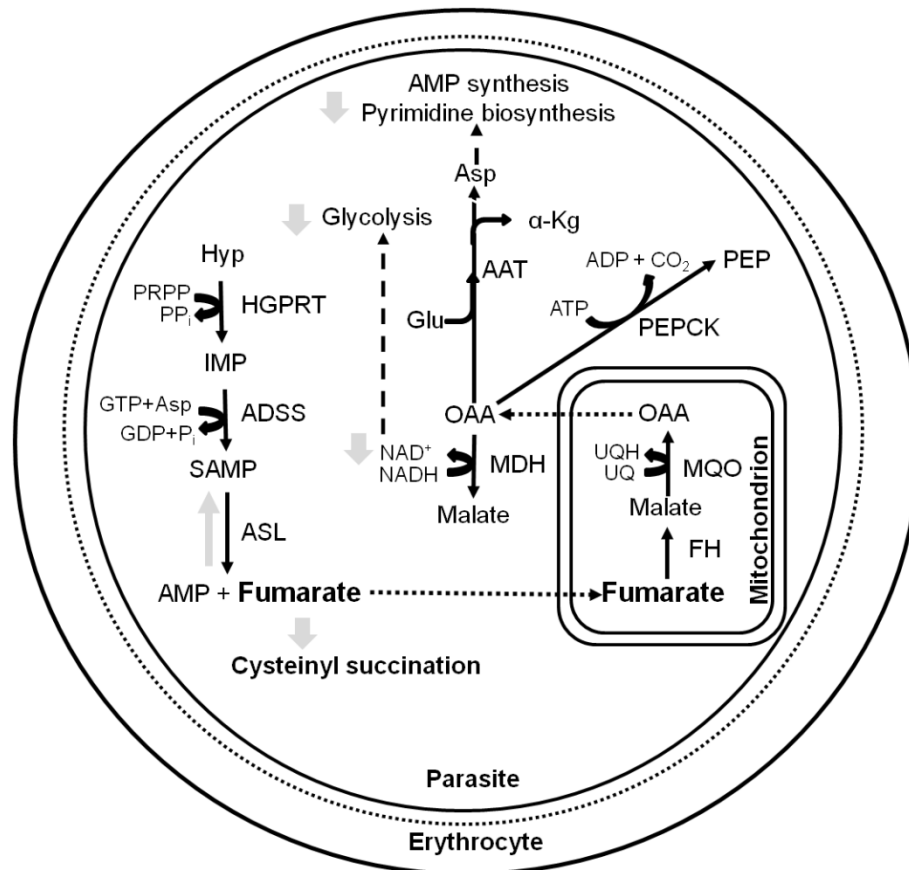


**Figure 7. The metabolic consequences of fumarate hydratase gene deletion in *Plasmodium*.** Dashed arrows indicate flow of metabolites into a pathway while dotted arrows indicate transport across compartments. Grey arrows show possible metabolic consequences of *fh* gene deletion. AAT, aspartate aminotransferase, ADSS, adenylosuccinate synthetase, ASL, adenylosuccinate lyase, FH, fumarate hydratase, HGPRT, hypoxanthine guanine phosphoribosyltransferase, MDH, malate dehydrogenase, MQO, malate-quinone oxidoreductase, PEPCK, phosphoenolpyruvate carboxykinase,  $\alpha$ -Kg,  $\alpha$ -ketoglutarate, AMP, adenosine 5'-monophosphate, Asp, aspartic acid, Glu, glutamic acid, Hyp, hypoxanthine, OAA, oxaloacetate, PEP, phosphoenolpyruvate, PRPP, phosphoribosyl 5'-pyrophosphate, SAMP, succinyl-AMP, UQ, ubiquinone, UQH, ubiquinol.

Attempts at knockdown of P<sub>f</sub>FH levels in FH-GFP strain where FH is fused to EcDHFR degradation domain did not result in lowering of protein levels. It has been shown that proteins targeted to organelles are not degraded through the proteasomal machinery making this approach unsuitable for knockdown of non-cytosolic proteins. Knockout of *fh* in *P. berghei* using BALB/c strain of mice yielded parasites that showed insertion of the marker cassette with the retention of the functional copy of the gene suggesting its essentiality for the intra-erythrocytic

stages. The major source of intracellular fumarate in *Plasmodium* is from the synthesis of AMP. From the context of metabolism, the absence of fumarate hydratase would result in the accumulation of fumarate. The possible metabolic consequences of this are schematically shown in **Figure 7**. The last reaction in AMP synthesis catalyzed by ASL is a reversible process with similar catalytic efficiencies for the forward and reverse reactions. Accumulation of fumarate could lead to an increased flux through the reverse reaction catalyzed by ASL resulting in accumulation of sAMP and lowered levels of AMP, eventually resulting in compromised cell growth. Subversion of ASL activity through the use of AICAR has been shown to result in parasite death (54). Apart from perturbing AMP synthesis, high levels of fumarate, can result in succination of cysteinyl residues in proteins and glutathione (55) thereby, compromising cellular homeostasis (56). Succinated proteome in human cell lines (57–59) and *Mycobacterium tuberculosis* (60) have been examined and these highlight the toxic effects of high levels of fumarate. Fumarate is recycled to aspartate through the action of enzymes, FH, MQO and AAT. In the absence of FH, the levels of malate and oxaloacetate intermediates in this pathway would be perturbed leading to lower levels of recycling. Further, with lowered levels of OAA due to the absence of FH, the generation of NAD<sup>+</sup> through MDH would also be impaired due to absence of FH. All these biochemical requirements could make FH in *Plasmodium* essential.

## ACKNOWLEDGEMENTS

This project was funded by DBT (BT/PR11294/BRB/10/1291/2014 and BT/PR13760/COE/34/42/2015), SERB (EMR/2014/001276) and institutional funding from JNCASR. VJ acknowledges CSIR for junior and senior research fellowships. AS acknowledges UGC for junior and senior research fellowships.

## REFERENCES

1. Roth, E. (1990) *Plasmodium falciparum* carbohydrate metabolism: a connection between host cell and parasite. *Blood Cells*. **16**, 453-60–6
2. MacRae, J. I., Dixon, M. W., Dearnley, M. K., Chua, H. H., Chambers, J. M., Kenny, S., Bottova, I., Tilley, L., and McConville, M. J. (2013) Mitochondrial metabolism of sexual and asexual blood stages of the malaria parasite *Plasmodium falciparum*. *BMC Biol.* **11**, 67

3. Bulusu, V., Jayaraman, V., and Balaram, H. (2011) Metabolic fate of fumarate, a side product of the purine salvage pathway in the intraerythrocytic stages of *Plasmodium falciparum*. *J. Biol. Chem.* **286**, 9236–9245
4. Teipel, J. W., Hass, G. M., and Hill, R. L. (1968) The substrate specificity of fumarase. *J. Biol. Chem.* **243**, 5684–94
5. Chen, B.-S., Otten, L. G., and Hanefeld, U. (2015) Stereochemistry of enzymatic water addition to C=C bonds. *Biotechnol. Adv.* **33**, 526–546
6. Resch, V., and Hanefeld, U. (2015) The selective addition of water. *Catal. Sci. Technol.* **5**, 1385–1399
7. Woods, S. A., Schwartzbach, S. D., and Guest, J. R. (1988) Two biochemically distinct classes of fumarase in *Escherichia coli*. *Biochim. Biophys. Acta.* **954**, 14–26
8. Shimoyama, T., Rajashekhara, E., Ohmori, D., Kosaka, T., and Watanabe, K. (2007) MmcBC in *Pelotomaculum thermopropionicum* represents a novel group of prokaryotic fumarases. *FEMS Microbiol. Lett.* **270**, 207–13
9. Flint, D. H. (1994) Initial Kinetic and Mechanistic Characterization of *Escherichia coli* Fumarase A. *Arch. Biochem. Biophys.* **311**, 509–516
10. Kronen, M., Sasikaran, J., and Berg, I. A. (2015) Mesoconase Activity of Class I Fumarase Contributes to Mesoconate Utilization by *Burkholderia xenovorans*. *Appl. Environ. Microbiol.* **81**, 5632–5638
11. Feliciano, P. R., Drennan, C. L., and Nonato, M. C. (2016) Crystal structure of an Fe-S cluster-containing fumarate hydratase enzyme from *Leishmania major* reveals a unique protein fold. *Proc. Natl. Acad. Sci.* **113**, 9804–9809
12. Beinert, H., Kennedy, M. C., and Stout, C. D. (1996) Aconitase as Iron–Sulfur Protein, Enzyme, and Iron-Regulatory Protein. *Chem. Rev.* **96**, 2335–2374
13. Lloyd, S. J., Lauble, H., Prasad, G. S., and Stout, C. D. (1999) The mechanism of aconitase: 1.8 Å resolution crystal structure of the S642a:citrate complex. *Protein Sci.* **8**, 2655–62
14. Kronen, M., and Berg, I. A. (2015) Mesoconase/Fumarase FumD in *Escherichia coli* O157:H7 and Promiscuity of *Escherichia coli* Class I Fumarases FumA and FumB. *PLoS One.* **10**, e0145098
15. Sacchettini, J. C., Meininger, T., Roderick, S., and Banaszak, L. J. (1986) Purification, crystallization, and preliminary X-ray data for porcine fumarase. *J. Biol. Chem.* **261**, 15183–5
16. Weaver, T. M., Levitt, D. G., and Banaszak, L. J. (1993) Purification and Crystallization of Fumarase C from *Escherichia coli*. *J. Mol. Biol.* **231**, 141–144
17. Weaver, T., Lees, M., Zaitsev, V., Zaitseva, I., Duke, E., Lindley, P., McSweeney, S., Svensson, A., Keruchenko, J., Keruchenko, I., Gladilin, K., and

- Banaszak, L. (1998) Crystal structures of native and recombinant yeast fumarase. *J. Mol. Biol.* **280**, 431–42
18. Weaver, T. (2005) Structure of free fumarase C from *Escherichia coli*. *Acta Crystallogr. D. Biol. Crystallogr.* **61**, 1395–401
19. Pereira de Pádua, R. A., and Nonato, M. C. (2014) Cloning, expression, purification, crystallization and preliminary X-ray diffraction analysis of recombinant human fumarase. *Acta Crystallogr. Sect. F Struct. Biol. Commun.* **70**, 120–122
20. Jacot, D., Waller, R. F., Soldati-Favre, D., MacPherson, D. A., and MacRae, J. I. (2016) Apicomplexan Energy Metabolism: Carbon Source Promiscuity and the Quiescence Hyperbole. *Trends Parasitol.* **32**, 56–70
21. Feliciano, P. R., Gupta, S., Dyszy, F., Dias-Baruffi, M., Costa-Filho, A. J., Michels, P. A. M., and Nonato, M. C. (2012) Fumarate hydratase isoforms of *Leishmania major*: Subcellular localization, structural and kinetic properties. *Int. J. Biol. Macromol.* **51**, 25–31
22. de Pádua, R. A. P., Kia, A. M., Costa-Filho, A. J., Wilkinson, S. R., and Nonato, M. C. (2017) Characterisation of the fumarate hydratase repertoire in *Trypanosoma cruzi*. *Int. J. Biol. Macromol.* **102**, 42–51
23. Ke, H., Lewis, I. A., Morrissey, J. M., McLean, K. J., Ganesan, S. M., Painter, H. J., Mather, M. W., Jacobs-Lorena, M., Llinás, M., Vaidya, A. B. (2015) Genetic investigation of tricarboxylic acid metabolism during the *Plasmodium falciparum* life cycle. *Cell Rep.* **11**, 164–174
24. Carey, M. A., Papin, J. A., and Guler, J. (2017) Novel *Plasmodium falciparum* metabolic network reconstruction identifies shifts associated with clinical antimalarial resistance. *bioRxiv*
25. Altschul, S. F., Gish, W., Miller, W., Myers, E. W., and Lipman, D. J. (1990) Basic local alignment search tool. *J. Mol. Biol.* **215**, 403–10
26. Muralidharan, V., Oksman, A., Iwamoto, M., Wandless, T. J., and Goldberg, D. E. (2011) Asparagine repeat function in a *Plasmodium falciparum* protein assessed via a regulatable fluorescent affinity tag. *Proc. Natl. Acad. Sci. U. S. A.* **108**, 4411–4416
27. Baba, T., Ara, T., Hasegawa, M., Takai, Y., Okumura, Y., Baba, M., Datsenko, K. A., Tomita, M., Wanner, B. L., and Mori, H. (2006) Construction of *Escherichia coli* K-12 in-frame, single-gene knockout mutants: the Keio collection. *Mol. Syst. Biol.* **2**, 2006.0008
28. Datsenko, K. A., and Wanner, B. L. (2000) One-step inactivation of chromosomal genes in *Escherichia coli* K-12 using PCR products. *Proc. Natl. Acad. Sci. U. S. A.* **97**, 6640–5
29. Yamamoto, N., Nakahigashi, K., Nakamichi, T., Yoshino, M., Takai, Y.,

- Touda, Y., Furubayashi, A., Kinjyo, S., Dose, H., Hasegawa, M., Datsenko, K. A., Nakayashiki, T., Tomita, M., Wanner, B. L., and Mori, H. (2009) Update on the Keio collection of *Escherichia coli* single-gene deletion mutants. *Mol. Syst. Biol.* **5**, 335
30. Trager, W., and Jensen, J. B. (1976) Human malaria parasites in continuous culture. *Science.* **193**, 673–5
31. Rug, M., and Maier, A. G. (2013) Transfection of *Plasmodium falciparum*. *Methods Mol. Biol.* **923**, 75–98
32. Abràmoff.M.D., Magalhães P.J., R. S. J. (2004) Image Processing with ImageJ. *Biophotonics Int.* **11**, 36–42
33. Hartig, S. M. (2013) Basic Image Analysis and Manipulation in ImageJ. in *Current Protocols in Molecular Biology*, p. Unit14.15, John Wiley & Sons, Inc., Hoboken, NJ, USA, Chapter 14, Unit14.15
34. Pfander, C., Anar, B., Schwach, F., Otto, T. D., Brochet, M., Volkmann, K., Quail, M. A., Pain, A., Rosen, B., Skarnes, W., Rayner, J. C., and Billker, O. (2011) A scalable pipeline for highly effective genetic modification of a malaria parasite. *Nat. Methods.* **8**, 1078–1082
35. Janse, C. J., Ramesar, J., and Waters, A. P. (2006) High-efficiency transfection and drug selection of genetically transformed blood stages of the rodent malaria parasite *Plasmodium berghei*. *Nat. Protoc.* **1**, 346–356
36. Oborník, M., Modrý, D., Lukeš, M., Černotíková-Stříbrná, E., Cihlář, J., Tesařová, M., Kotabová, E., Vancová, M., Prášil, O., and Lukeš, J. (2012) Morphology, Ultrastructure and Life Cycle of *Vitrella brassicaformis* n. sp., n. gen., a Novel Chromerid from the Great Barrier Reef. *Protist.* **163**, 306–323
37. Fukasawa, Y., Tsuji, J., Fu, S.-C., Tomii, K., Horton, P., and Imai, K. (2015) MitoFates: Improved Prediction of Mitochondrial Targeting Sequences and Their Cleavage Sites . *Mol. Cell. Proteomics.* **14**, 1113–1126
38. Woo, Y. H., Ansari, H., Otto, T. D., Klinger, C. M., Kolisko, M., Michálek, J., Saxena, A., Shanmugam, D., Tayyrov, A., Veluchamy, A., Ali, S., Bernal, A., del Campo, J., Cihlář, J., Flegontov, P., Gornik, S. G., Hajdušková, E., Horák, A., Janouškovec, J., Katris, N. J., Mast, F. D., Miranda-Saavedra, D., Mourier, T., Naeem, R., Nair, M., Panigrahi, A. K., Rawlings, N. D., Padron-Regalado, E., Ramaprasad, A., Samad, N., Tomčala, A., Wilkes, J., Neafsey, D. E., Doerig, C., Bowler, C., Keeling, P. J., Roos, D. S., Dacks, J. B., Templeton, T. J., Waller, R. F., Lukeš, J., Oborník, M., and Pain, A. (2015) Chromerid genomes reveal the evolutionary path from photosynthetic algae to obligate intracellular parasites. *Elife.* **4**, e06974
39. Bender, A., van Dooren, G. G., Ralph, S. A., McFadden, G. I., and Schneider, G. (2003) Properties and prediction of mitochondrial transit peptides from



*Plasmodium falciparum*. *Mol. Biochem. Parasitol.* **132**, 59–66

40. Bell, P. J., Andrews, S. C., Sivak, M. N., and Guest, J. R. (1989) Nucleotide sequence of the FNR-regulated fumarase gene (*fumB*) of *Escherichia coli* K-12. *J. Bacteriol.* **171**, 3494–3503
41. Jervis, A. J., Crack, J. C., White, G., Artymiuk, P. J., Cheesman, M. R., Thomson, A. J., Le Brun, N. E., and Green, J. (2009) The O<sub>2</sub> sensitivity of the transcription factor FNR is controlled by Ser24 modulating the kinetics of [4Fe-4S] to [2Fe-2S] conversion. *Proc. Natl. Acad. Sci. U. S. A.* **106**, 4659–64
42. Crack, J. C., Smith, L. J., Stapleton, M. R., Peck, J., Watmough, N. J., Buttner, M. J., Buxton, R. S., Green, J., Oganessian, V. S., Thomson, A. J., and Le Brun, N. E. (2011) Mechanistic Insight into the Nitrosylation of the [4Fe-4S] Cluster of WhiB-like Proteins. *J. Am. Chem. Soc.* **133**, 1112–1121
43. Crack, J. C., Stapleton, M. R., Green, J., Thomson, A. J., and Le Brun, N. E. (2013) Mechanism of [4Fe-4S](Cys)<sub>4</sub> cluster nitrosylation is conserved among NO-responsive regulators. *J. Biol. Chem.* **288**, 11492–502
44. Nakamaru-Ogiso, E., Yano, T., Ohnishi, T., and Yagi, T. (2002) Characterization of the iron-sulfur cluster coordinated by a cysteine cluster motif (CXXCXXXCX<sub>2</sub>7C) in the Nqo3 subunit in the proton-translocating NADH-quinone oxidoreductase (NDH-1) of *Thermus thermophilus* HB-8. *J. Biol. Chem.* **277**, 1680–8
45. van Vugt-Lussenburg, B. M. A., van der Weel, L., Hagen, W. R., and Hagedoorn, P.-L. (2013) Biochemical similarities and differences between the catalytic [4Fe-4S] cluster containing fumarases FumA and FumB from *Escherichia coli*. *PLoS One.* **8**, e55549
46. van Vugt-Lussenburg, B. M. A., van der Weel, L., Hagen, W. R., and Hagedoorn, P.-L. (2009) Identification of two [4Fe-4S]-cluster-containing hydrolyases from *Pyrococcus furiosus*. *Microbiology.* **155**, 3015–20
47. Chan, A., Clémancey, M., Mouesca, J.-M., Amara, P., Hamelin, O., Latour, J.-M., and Ollagnier de Choudens, S. (2012) Studies of Inhibitor Binding to the [4Fe-4S] Cluster of Quinolate Synthase. *Angew. Chemie Int. Ed.* **51**, 7711–7714
48. Ueda, Y., Yumoto, N., Tokushige, M., Fukui, K., and Ohya-Nishiguchi, H. (1991) Purification and characterization of two types of fumarase from *Escherichia coli*. *J. Biochem.* **109**, 728–33
49. Gomes, A. R., Bushell, E., Schwach, F., Girling, G., Anar, B., Quail, M. A., Herd, C., Pfander, C., Modrzynska, K., Rayner, J. C., and Billker, O. (2015) A genome-scale vector resource enables high-throughput reverse genetic screening in a malaria parasite. *Cell Host Microbe.* **17**, 404–13
50. Guler, J. L., Freeman, D. L., Ah Yong, V., Patrapuvich, R., White, J., Gujjar, R., Phillips, M. A., DeRisi, J., and Rathod, P. K. (2013) Asexual Populations of the

Human Malaria Parasite, *Plasmodium falciparum*, Use a Two-Step Genomic Strategy to Acquire Accurate, Beneficial DNA Amplifications. *PLoS Pathog.* **9**, e1003375

51. Niikura, M., Komatsuya, K., Inoue, S.-I., Matsuda, R., Asahi, H., Inaoka, D. K., Kita, K., and Kobayashi, F. (2017) Suppression of experimental cerebral malaria by disruption of malate:quinone oxidoreductase. *Malar. J.* **16**, 247

52. Brandt, U., Waletzko, C., Voigt, B., Hecker, M., and Steinbüchel, A. (2014) Mercaptosuccinate metabolism in *Variovorax paradoxus* strain B4—a proteomic approach. *Appl. Microbiol. Biotechnol.* **98**, 6039–6050

53. Brandt, U., Schürmann, M., and Steinbüchel, A. (2014) Mercaptosuccinate Dioxygenase, a Cysteine Dioxygenase Homologue, from *Variovorax paradoxus* Strain B4 Is the Key Enzyme of Mercaptosuccinate Degradation. *J. Biol. Chem.* **289**, 30800–30809

54. Bulusu, V., Thakur, S. S., Venkatachala, R., and Balaram, H. (2011) Mechanism of growth inhibition of intraerythrocytic stages of *Plasmodium falciparum* by 5-aminoimidazole-4-carboxamide ribonucleoside (AICAR). *Mol. Biochem. Parasitol.* **177**, 1–11

55. Alderson, N. L., Wang, Y., Blatnik, M., Frizzell, N., Walla, M. D., Lyons, T. J., Alt, N., Carson, J. A., Nagai, R., Thorpe, S. R., and Baynes, J. W. (2006) S-(2-Succinyl)cysteine: A novel chemical modification of tissue proteins by a Krebs cycle intermediate. *Arch. Biochem. Biophys.* **450**, 1–8

56. Sullivan, L., Martinez-Garcia, E., Nguyen, H., Mullen, A., Dufour, E., Sudarshan, S., Licht, J., Deberardinis, R., and Chandel, N. (2013) The Proto-oncometabolite Fumarate Binds Glutathione to Amplify ROS-Dependent Signaling. *Mol. Cell.* **51**, 236–248

57. Frizzell, N., Rajesh, M., Jepson, M. J., Nagai, R., Carson, J. A., Thorpe, S. R., and Baynes, J. W. (2009) Succination of Thiol Groups in Adipose Tissue Proteins in Diabetes: Succination inhibits polymerization and secretion of adiponectin. *J. Biol. Chem.* **284**, 25772–25781

58. Merkley, E. D., Metz, T. O., Smith, R. D., Baynes, J. W., and Frizzell, N. (2014) The succinated proteome. *Mass Spectrom. Rev.* **33**, 98–109

59. Yang, M., Ternette, N., Su, H., Dabiri, R., Kessler, B., Adam, J., Teh, B., and Pollard, P. (2014) The Succinated Proteome of FH-Mutant Tumours. *Metabolites.* **4**, 640–654

60. Ruecker, N., Jansen, R., Trujillo, C., Puckett, S., Jayachandran, P., Piroli, G. G., Frizzell, N., Molina, H., Rhee, K. Y., and Ehrt, S. (2017) Fumarase Deficiency Causes Protein and Metabolite Succination and Intoxicates *Mycobacterium tuberculosis*. *Cell Chem. Biol.* **24**, 306–315